



A dual role for hepatocyte-intrinsic canonical NF- B signaling in virus control

Namineni, Sukumar ; O'Connor, Tracy ; Faure-Dupuy, Suzanne ; Johansen, Pål ; Lenggenhager, Daniela ; et al ; Weber, Achim

Abstract: BACKGROUND AIMS Hepatic innate immune control of viral infections has largely been attributed to Kupffer cells, the liver macrophages. However, also hepatocytes, the parenchymal cells of the liver, possess potent immunological functions in addition to their known metabolic functions. Owing to their abundance in the liver and known immunological functions, we aimed to investigate the direct anti-viral mechanisms employed by hepatocytes. METHODS Using lymphocytic choriomeningitis virus (LCMV) as a model of liver infection, we first assessed the role of myeloid cells by depletion prior to infection. We investigated the role of hepatocyte-intrinsic innate immune signaling by infecting mice lacking canonical NF- B signaling (IKK^{Hep}) specifically in hepatocytes. In addition, mice lacking hepatocyte-specific interferon- / signaling-(IFNAR^{Hep}), or interferon- / signaling in myeloid cells-(IFNAR^{Myel}) were infected. RESULTS Here, we demonstrate that LCMV activates NF- B signaling in hepatocytes. LCMV-triggered NF- B activation in hepatocytes did not depend on Kupffer cells or TNFR1- but rather on TLR-signaling. LCMV-infected IKK^{Hep} livers displayed strongly elevated viral titers due to LCMV accumulation within hepatocytes, reduced interferon-stimulated gene (ISG) expression, delayed intra-hepatic immune cell influx and delayed intrahepatic LCMV-specific CD8⁺ T-cell responses. Notably, viral clearance and ISG expression were also reduced in LCMV-infected primary hepatocytes lacking IKK, demonstrating a hepatocyte-intrinsic effect. Similar to livers of IKK^{Hep} mice, enhanced hepatocytic LCMV accumulation was observed in livers of IFNAR^{Hep}, whereas IFNAR^{Myel} mice were able to control LCMV-infection. Hepatocytic NF- B signaling was also required for efficient ISG induction in HDV-infected dHepaRG cells and interferon- / -mediated inhibition of HBV replication in vitro. CONCLUSIONS Together, these data show that hepatocyte-intrinsic NF- B is a vital amplifier of interferon- / signaling pivotal for early, strong ISG responses, influx of immune cells and hepatic viral clearance.

DOI: <https://doi.org/10.1016/j.jhep.2019.12.019>

Posted at the Zurich Open Repository and Archive, University of Zurich

ZORA URL: <https://doi.org/10.5167/uzh-186502>

Journal Article

Accepted Version

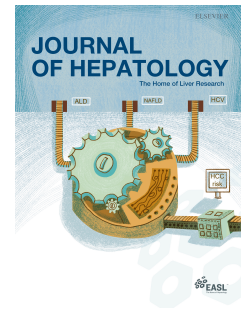


The following work is licensed under a Creative Commons: Attribution-NonCommercial-NoDerivatives 4.0 International (CC BY-NC-ND 4.0) License.

Originally published at:

Namineni, Sukumar; O'Connor, Tracy; Faure-Dupuy, Suzanne; Johansen, Pål; Lenggenger, Daniela; et al; Weber, Achim (2020). A dual role for hepatocyte-intrinsic canonical NF- B signaling in virus control. *Journal of Hepatology*, 72(5):960-975.
DOI: <https://doi.org/10.1016/j.jhep.2019.12.019>

Journal Pre-proof



A dual role for hepatocyte-intrinsic canonical NF- κ B signaling in virus control

Sukumar Namineni, Tracy O'Connor, Suzanne Faure-Dupuy, Pål Johansen, Tobias Riedl, Kaijing Liu, Haifeng Xu, Indrabahadur Singh, Prashant Shinde, Fanghui Li, Aleksandra Pandyra, Piyush Sharma, Marc Ringelhan, Andreas Muschaweckh, Katharina Borst, Patrick Blank, Sandra Lampl, David Durantel, Rayan Farhat, Achim Weber, Daniela Lenggenhager, Thomas M. Kündig, Peter Staeheli, Ulrike Protzer, Dirk Wohlleber, Bernhard Holzmann, Marco Binder, Kai Breuhahn, Lisa Mareike Assmus, Jacob Nattermann, Zeinab Abdullah, Maude Rolland, Emmanuel Dejardin, Philipp A. Lang, Karl S. Lang, Michael Karin, Julie Lucifora, Ulrich Kalinke, Percy A. Knolle, Mathias Heikenwalder

PII: S0168-8278(20)30010-6

DOI: <https://doi.org/10.1016/j.jhep.2019.12.019>

Reference: JHEPAT 7580

To appear in: *Journal of Hepatology*

Received Date: 6 May 2019

Revised Date: 2 December 2019

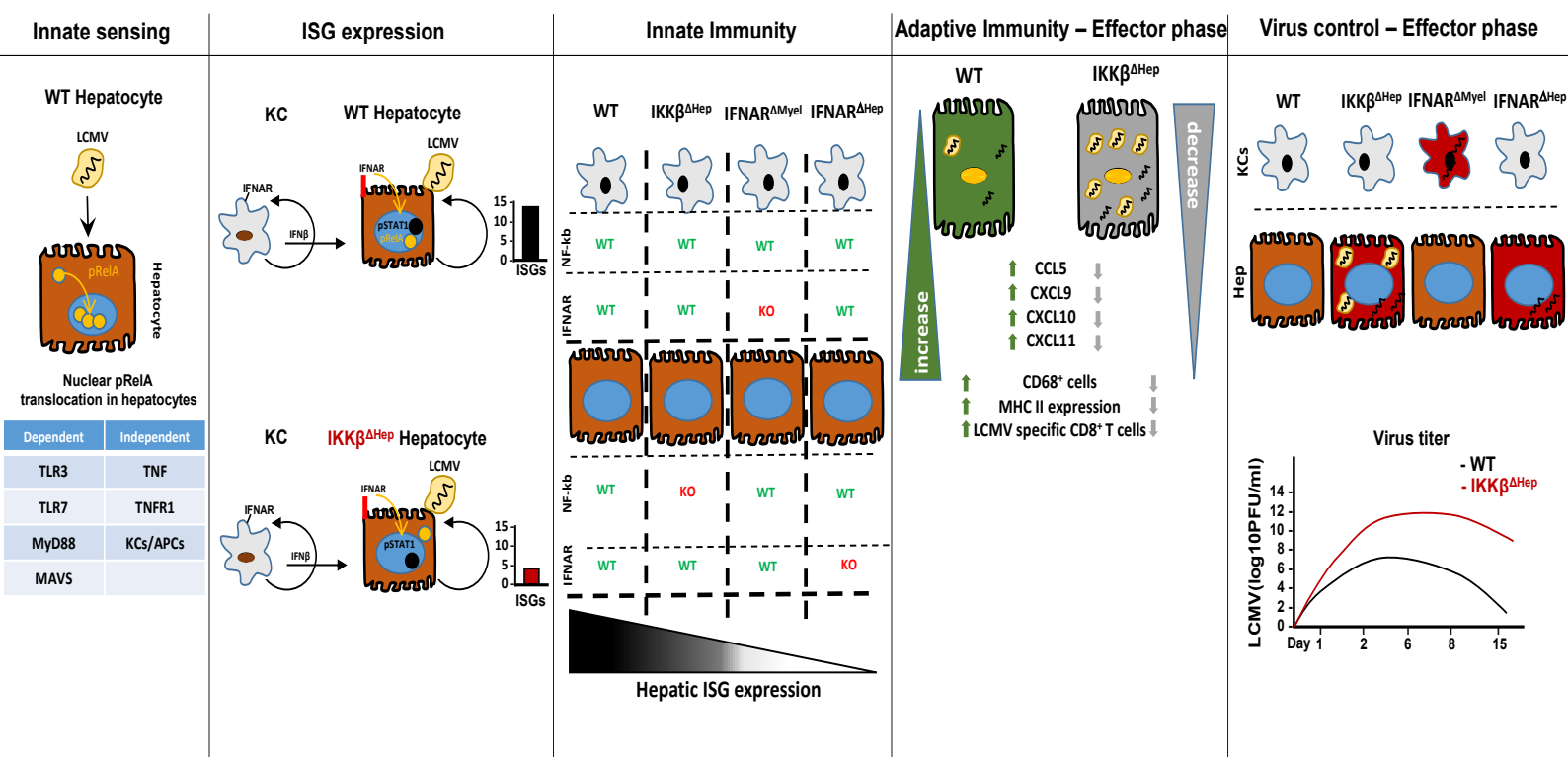
Accepted Date: 11 December 2019

Please cite this article as: Namineni S, O'Connor T, Faure-Dupuy S, Johansen P, Riedl T, Liu K, Xu H, Singh I, Shinde P, Li F, Pandyra A, Sharma P, Ringelhan M, Muschaweckh A, Borst K, Blank P, Lampl S, Durantel D, Farhat R, Weber A, Lenggenhager D, Kündig TM, Staeheli P, Protzer U, Wohlleber D, Holzmann B, Binder M, Breuhahn K, Assmus LM, Nattermann J, Abdullah Z, Rolland M, Dejardin E, Lang PA, Lang KS, Karin M, Lucifora J, Kalinke U, Knolle PA, Heikenwalder M, A dual role for hepatocyte-intrinsic canonical NF- κ B signaling in virus control, *Journal of Hepatology* (2020), doi: <https://doi.org/10.1016/j.jhep.2019.12.019>.

This is a PDF file of an article that has undergone enhancements after acceptance, such as the addition of a cover page and metadata, and formatting for readability, but it is not yet the definitive version of record. This version will undergo additional copyediting, typesetting and review before it is published in its final form, but we are providing this version to give early visibility of the article. Please note that,

during the production process, errors may be discovered which could affect the content, and all legal disclaimers that apply to the journal pertain.

© 2020 Published by Elsevier B.V. on behalf of European Association for the Study of the Liver.



Namineni et al. Fig. 7

A dual role for hepatocyte-intrinsic canonical NF- κ B signaling in virus control

Sukumar Namineni^{1,2,3}, Tracy O'Connor^{1,3,*}, Suzanne Faure-Dupuy^{1,*}, Pål Johansen⁴, Tobias Riedl¹, Kaijing Liu⁵, Haifeng Xu⁶, Indrabahadur Singh⁷, Prashant Shinde⁸, Fanghui Li⁶, Aleksandra Pandya⁶, Piyush Sharma^{6,9}, Marc Ringelhan^{1,2,10}, Andreas Muschaweckh¹¹, Katharina Borst¹², Patrick Blank¹², Sandra Lampl³, David Durantel¹³, Rayan Farhat¹³, Achim Weber¹⁴, Daniela Lenggenhager¹⁴, Thomas M. Kündig⁴, Peter Staeheli¹⁵, Ulrike Protzer^{1,2}, Dirk Wohlleber³, Bernhard Holzmann¹⁶, Marco Binder¹⁷, Kai Breuhahn⁵, Lisa Mareike Assmus¹⁸, Jacob Nattermann¹⁹, Zeinab Abdullah¹⁸, Maude Rolland²⁰, Emmanuel Dejardin²⁰, Philipp A. Lang⁸, Karl S. Lang⁶, Michael Karin²¹, Julie Lucifora¹³, Ulrich Kalinke¹², Percy A. Knolle³, Mathias Heikenwalder^{1,2,3†}

¹Division of Chronic Inflammation and Cancer, German Cancer Research Center (DKFZ), Heidelberg, Germany.

²Institute of Virology, Technical University of Munich and Helmholtz Zentrum München, Schneckenerstrasse 8, 81675 Munich, Germany

³Institute of Molecular Immunology and Experimental Oncology, Technical University of Munich, Ismaningerstraße 22, 81675 Munich, Germany

⁴Department of Dermatology, University Hospital Zurich and University of Zurich, Gloriastrasse 31, 8091 Zurich, Switzerland.

⁵Institute of Pathology, University Hospital Heidelberg, Heidelberg, Germany.

⁶Institute of Immunology, Medical Faculty, University of Duisburg-Essen, Hufelandstr. 55, Essen 45147, Germany.

⁷Emmy Noether Research Group Epigenetic Machineries and Cancer, Division of Chronic Inflammation and Cancer, German Cancer Research Center (DKFZ), Heidelberg, Germany.

⁸Department of Molecular Medicine II, Medical Faculty, Heinrich Heine University, Universitätsstr. 1, 40225 Düsseldorf, Germany.

⁹Department of Immunology, St. Jude Children's Research Hospital, Memphis, TN, USA, 38105

¹⁰Department of Internal Medicine II, University Hospital rechts der Isar, Technical University of Munich, Ismaninger Str. 22, 81675 Munich, Germany

¹¹Klinikum rechts der Isar, Department of Neurology, Technical University of Munich, Ismaninger Str. 22, 81675 Munich, Germany

¹²Institute for Experimental Infection Research, TWINCORE, Centre for Experimental and Clinical Infection Research, a joint venture between the Hanover Medical School and the Helmholtz Centre for Infection Research, Brunswick, Germany.

¹³INSERM, U1052, Cancer Research Center of Lyon (CRCL), Université de Lyon (UCBL1), CNRS UMR 5286, Centre Léon Bérard, Lyon, France

¹⁴Department of Pathology and Molecular Pathology, University Hospital of Zurich, 8091 Zurich, Switzerland.

¹⁵Institute of Virology, University of Freiburg, Freiburg, Germany.

¹⁶Department of Surgery, Klinikum rechts der Isar, Technische Universität München, Munich, Germany.

¹⁷Research Group "Dynamics of Early Viral Infection and the Innate Antiviral Response", Division Virus-Associated Carcinogenesis (F170), German Cancer Research Center (DKFZ), 69120 Heidelberg, Germany.

¹⁸Institute of Experimental Immunology, Bonn, Germany

¹⁹Department of Internal Medicine, University of Bonn, Bonn, Germany

²⁰Laboratory of Molecular Immunology and Signal Transduction, GIGA-Institute, University of Liège, 4000 Liège, Belgium.

²¹Laboratory of Gene Regulation and Signal Transduction, Department of Pharmacology, School of Medicine, University of California San Diego (UCSD), 9500 Gilman Drive, La Jolla, California 92093, USA

*Contributed equally

†Corresponding Author:

Prof. Dr. Mathias Heikenwälder

Division Chronic Inflammation and Cancer (F180), German Cancer Research Center (DKFZ), Im Neuenheimer Feld 242, 69120 Heidelberg, Germany.

Tel.: +49 6221 42-3891

Fax: +49 6221 42-3899

Email: m.heikenwaelder@dkfz-heidelberg.de

Key words: Hepatocytes, Innate Immune responses, NF-kB signaling, PRRs, Interferon Stimulated Genes, Cytotoxic T cells

Electronic word count of the main text: 9057

Number of figures: 6

Number of supplementary figures: 6

Number of tables: 4

Conflict of interest statement

The following authors declare no competing financial interests: S.N., T.O., S.F.D, P.J., T.R., K.L., H.X., I.S., P.S., F.L., A.P., P.Sh., M.R., A.M., K.B., P.B., S.L., D.D., R.F., A.W., D.L., T.K., P.St., U.P., D.W., B.H., M.B., K.B., L.M.A., J.N., Z.A., M.R., E.D., P.L., K.L., M.K., J.L., U.K., P.K., M.H.

Financial support statement

This manuscript was supported by the SFBTR179 and 209 to M.H., U.P., P.K. and M.B. M.H. was supported by an ERC consolidator grant (HeptoMetaboPath), the EOS grant (Flundern) and a Horizon 2020 grant. I.S. was supported by an Emmy Noether Program.

Author contributions

M.H., S.N. and T.O. conceived the study. S.N., T.O., S.F.D. and M.H. designed all the experiments. S.N., T.O., S.F.D., P.J., T.R., K.L., H.X., I.S., P.S., F.L., A.P., P.Sh., M.R., A.M., K.B., P.B., S.K., R.F., D.L., P.St., D.W., Z.A., M.R., J.L., L.M.A. performed experiments. S.N., T.O., S.F.D., and M.H. wrote the manuscript. T.O. co-supervised the study. P.K. gave critical inputs to the study, provided reagents and performed experiments together with D.W., S.K., J.N. and Z.A., D.D., A.W., T.K., U.P., B.H., M.B., K.Br., E.D., P.L., K.L., M.K., U.K. and all authors contributed to the development of the manuscript.

Abstract

Background & Aims: Hepatic innate immune control of viral infections has largely been attributed to Kupffer cells, the liver macrophages. However, also hepatocytes, the parenchymal cells of the liver, possess potent immunological functions in addition to their known metabolic functions. Owing to their abundance in the liver and known immunological functions, we aimed to investigate the direct anti-viral mechanisms employed by hepatocytes.

Methods: Using lymphocytic choriomeningitis virus (LCMV) as a model of liver infection, we first assessed the role of myeloid cells by depletion prior to infection. We investigated the role of hepatocyte-intrinsic innate immune signaling by infecting mice lacking canonical NF- κ B signaling (IKK $\beta^{\Delta\text{Hep}}$) specifically in hepatocytes. In addition, mice lacking hepatocyte-specific interferon- α/β signaling-(IFNAR $^{\Delta\text{Hep}}$), or interferon- α/β signaling in myeloid cells-(IFNAR $^{\Delta\text{Myel}}$) were infected.

Results: Here, we demonstrate that LCMV activates NF- κ B signaling in hepatocytes. LCMV-triggered NF- κ B activation in hepatocytes did not depend on Kupffer cells or TNFR1- but rather on TLR-signaling. LCMV-infected IKK $\beta^{\Delta\text{Hep}}$ livers displayed strongly elevated viral titers due to LCMV accumulation within hepatocytes, reduced interferon-stimulated gene (ISG) expression, delayed intrahepatic immune cell influx and delayed intrahepatic LCMV-specific CD8 $^{+}$ T-cell responses. Notably, viral clearance and ISG expression were also reduced in LCMV-infected primary hepatocytes lacking IKK β , demonstrating a hepatocyte-intrinsic effect. Similar to livers of IKK $\beta^{\Delta\text{Hep}}$ mice, enhanced hepatocytic LCMV accumulation was observed in livers of IFNAR $^{\Delta\text{Hep}}$, whereas IFNAR $^{\Delta\text{Myel}}$ mice were able to control LCMV-infection. Hepatocytic NF- κ B signaling was also required for efficient ISG

1 induction in HDV-infected dHepaRG cells and interferon- α/β -mediated inhibition of
2 HBV replication *in vitro*.

3 **Conclusions:** Together, these data show that hepatocyte-intrinsic NF- κ B is a vital
4 amplifier of interferon- α/β signaling pivotal for early, strong ISG responses, influx of
5 immune cells and hepatic viral clearance.

6

7 **Lay summary**

8 Innate immune cells have been ascribed a primary role in controlling viral-clearance
9 upon hepatic infections. We identified a novel dual role for NF- κ B in infected
10 hepatocytes crucial for maximizing interferon responses and initiating adaptive
11 immunity, thereby efficiently controlling hepatic virus replication.

12

1 **Highlights**

- 2 • LCMV infection activates NF- κ B signaling in hepatocytes
- 3 • Macrophages, TNFR1 signaling do not induce LCMV-driven hepatocyte NF-
- 4 κ B-activation
- 5 • IKK $\beta^{\Delta\text{Hep}}$ mice display increased viral infection/replication and lower ISG
- 6 induction
- 7 • IFNAR $^{\Delta\text{Hep}}$ mice recapitulate aberrant virus replication as observed in IKK $\beta^{\Delta\text{Hep}}$
- 8 mice
- 9 • NF- κ B signaling is required for efficient ISG induction in HBV-/HDV-infected
- 10 HepaRG

1 Introduction

2 The liver is constantly exposed to pathogens coming from the gut via the hepatic
3 portal vein (1). Owing to this unique anatomical position, the liver not only serves as
4 a metabolic organ but also plays a central role in supporting innate and local
5 adaptive immunity (2). While maintaining immune tolerance, the liver continuously
6 removes a large and diverse spectrum of pathogens from the circulation, assuring
7 organ protection (3). The liver has the largest population of resident macrophages in
8 the whole body (3). Consequently, a sub-lethal bacterial inoculum in mice depleted
9 of liver resident macrophages (Kupffer cells; KCs) leads to increased bacterial load,
10 dissemination and death (4, 5), suggesting that the liver plays a non-redundant role
11 in conferring immunity to infections.

12 Hepatocytes are parenchymal cells of the liver encompassing ~80% of the entire
13 liver cell mass. In addition to being centrally involved in metabolic functions, plasma
14 protein expression and detoxification, hepatocytes are known to possess potent
15 immunological functions (6, 7). Several pathogen recognition receptors (PRRs) are
16 strongly expressed by hepatocytes (8). Upon encountering pathogen-associated
17 molecular patterns (PAMPs), hepatocytes readily secrete inflammatory cytokines,
18 which help control the spread and growth of pathogens (9). Owing to their
19 abundance in the liver and known immune functions, we aimed to investigate the
20 direct/indirect anti-viral mechanisms employed by hepatocytes.

21 Efficient clearance of a viral infection requires early detection of viral DNA or RNA by
22 pattern recognition receptors (PRRs) and induction of interferon responses, which
23 serves as the first line of defense. Interferons act by binding to type I interferon

1 receptors (IFNARs) on the cell surface initiating a signaling cascade by the JAK-
2 STAT pathway leading to the upregulation of interferon stimulated genes (ISGs).
3 Induction of ISG responses creates an effective cell-intrinsic antiviral state, which
4 restricts the replication of most viruses at an early stage (10).

5 Non-cytopathic lymphocytic choriomeningitis virus (LCMV-WE) is a negative-sense
6 single-stranded RNA virus belonging to the Arenaviridae family (11, 12). The
7 replication intermediates of this virus involve formation of dsRNA and 5'-PPP
8 structures, which are recognized by RIG-I and MDA5 activating IRF3 and NF- κ B-
9 mediated interferon responses (13, 14). While the downstream signaling from the
10 receptors of these stimuli might vary, in most of the cases, they all converge on the
11 activation of IKK (I κ B kinase) complex. The IKK complex consists of two catalytic
12 kinase subunits, IKK α and IKK β with intrinsic kinase activities and a regulatory
13 subunit, IKK γ , also known as NF- κ B essential modulator (NEMO) with helix-loop
14 helix and leucine-zipper motifs that mediate protein-protein interactions (15, 16). In
15 the inactive state p50:p65 dimers are held in the cytoplasm in association with the
16 inhibitors of kappaB (I κ B) proteins which mask the nuclear localization signal. The
17 activated IKK complex phosphorylates I κ B proteins at amino terminal serine residues
18 and marks them for ubiquitin-mediated proteasomal degradation, upon which NF- κ B
19 dimers translocate to the nucleus to bind DNA and enable gene transcription.

20 NF- κ B is activated by multiple viruses such as Human Immunodeficiency Virus,
21 Hepatitis C Virus, Rio Bravo Virus and influenza to enhance viral replication or
22 escape virus-induced apoptosis (17). Some viruses, such as VACV, encode proteins
23 with ankyrin repeats mimicking I κ B family proteins thereby inhibiting NF- κ B signaling
24 and subsequent immune responses (18). Furthermore, IKK β is essential for

1 induction of type I IFN and other inflammatory cytokines in response to a viral
2 infection (19).

3 To determine the relative contribution of hepatocytes to viral clearance in the liver,
4 we used a mouse model in which the essential upstream kinase in canonical NF- κ B
5 signaling, IKK β , was selectively deleted in hepatocytes by Cre recombinase-
6 mediated excision under the control of the albumin promoter - IKK $\beta^{\Delta\text{Hep}}$ mice (20-23).
7 These IKK $\beta^{\Delta\text{Hep}}$ mice were infected systemically with LCMV-WE strain. LCMV-WE
8 leads to an acute infection that is usually cleared within 2-3 weeks by virus-specific
9 CD8⁺ T cells. Intravenous infection in mice leads to infection of multiple visceral
10 organs such as lung, kidney, spleen, and liver (24, 25). Following a systemic
11 infection with LCMV in IKK $\beta^{\Delta\text{Hep}}$ mice, we analyzed the dynamics of viral replication
12 and clearance with a focus on the relative contribution of hepatocytes compared to
13 IFNAR $^{\Delta\text{Hep}}$, IFNAR $^{\Delta\text{Myel}}$, and wild-type (WT) livers. Our findings were corroborated in
14 differentiated HepaRG cells lacking IKK β either treated with IFN- α /TNF α or infected
15 with HDV. Our results highlight a central role of hepatocyte-intrinsic NF- κ B signaling
16 in supporting innate and adaptive immune responses to systemic viral infections.

17

Materials and Methods

Animals and infections

Alb-Cre transgenic mice expressing Cre recombinase from the hepatocyte-specific albumin promoter were crossed with $IKK\beta^{fl/fl}$ mice and $IFNAR^{fl/fl}$ mice to generate $IKK\beta^{\Delta Hep}$ mice and $IFNAR^{\Delta Hep}$ mice (20-22). LysM-Cre mice expressing Cre in myeloid cells due to a targeted insertion of the *cre* cDNA into their endogenous M lysozyme locus were crossed with $IFNAR^{fl/fl}$ mice to generate $IFNAR^{\Delta Myel}$ mice (26). To control the effects of Cre-induced cytotoxicity, histology was performed on livers obtained from C57BL/6 (WT), Alb-Cre, and $IKK\beta^{\Delta Hep}$ mice. No phenotypic differences were observed between WT and Alb-Cre mice. A total of 237 mice, of both male and female gender, were used in the experiments aged between 4 to 5 months. Each experiment has been performed with 3 to 6 mice. Mice used for experiments were maintained in single ventilated cages and under specific pathogen-free conditions. All mice used were of a C57BL/6/J genetic background. LCMV-WE was originally obtained from Rolf Zinkernagel (University Hospital Zurich (USZ), Switzerland) and propagated by infection of L929 fibroblast cells. Infection experiments were performed in Zurich under the licenses ZH 200/2006 and ZH 69/2012 as approved from the cantonal veterinary office of Zürich. Infection doses were given as indicated in each experiment, intravenously. At least 3-6 mice were used in each experimental group.

Clodronate treatment

Macrophages were depleted by injecting 200 μ l (~1 mg) of Clodronate-encapsulated liposomes (LIPOSOMA research, Cat no: CP-005-005 – 5 mg/ml formulation)

through the i.v. route in accordance with manufacturer's directions for administration (0.1 ml/10 g body mass). 200 µl of PBS-encapsulated liposomes were used as control. On day 2 post clodronate treatments, infections were carried out using LCMV (27).

LCMV nuclear protein (NP) immunofluorescence

5 µm liver cryo-sections on glass coverslips (ThermoFisher) from LCMV-infected mice were fixed in ice-cold 100% acetone for 10 min. Sections were then blocked for 15 min in 2% fetal calf serum (FCS; Hyclone) in PBS. Sections were then incubated overnight at 4° C in anti-LCMV NP supernatant (clone VL4) (24) diluted 1:4 in 2% FCS in PBS. Sections were washed in PBS and incubated for 1 h in 2 µg/ml AlexaFluor 488-conjugated goat anti-rat secondary antibody (Invitrogen) containing 1:10,000 DAPI in 2% FCS in PBS. Sections were then washed in PBS and mounted with fluorescent mounting medium (Dako), cover-slipped, and imaged using an Olympus BX53F fluorescent microscope or with a confocal Zeiss LSM 710 ConfoCor 3.

RelA immunofluorescence

5 µm liver cryo-sections on glass coverslips from LCMV-infected mice were fixed in 4% formalin for 10 min, washed in PBS for 2 min, and then washed for 10 min in PBS with 0.1% Tween 20 (PBST). Sections were then blocked for 1 h in 5% FCS and 0.25% Triton X-100 in PBS. Sections were then incubated at 4°C overnight in anti-RelA (NeoMarkers # RB-1638-P0) diluted 1:100 in 1% bovine serum albumin (BSA), 0.25% Triton-X 100 in PBS. Sections were then washed in PBS for 2 min., followed by PBST for 2 min, and incubated for 1 h in 4 µg/ml AlexaFluor 488-

conjugated goat anti-rabbit secondary antibody containing 1:10,000 DAPI in 1% BSA and 0.25% Triton-X 100 in PBS. Sections were then washed in PBS followed by 1x PBST, mounted with fluorescent mounting medium, cover-slipped, and imaged using an Olympus BX53F fluorescent microscope.

CD169 immunofluorescence

Histological analyses were performed on snap-frozen tissue as described previously (28). In brief, slides were fixed with Acetone for 10 min, incubated for 15 min in PBS and blocked with 2% FCS for 15 min. Sections were stained with rat anti-LCMV-NP antibody (clone VL4) and developed with FITC-anti-Rat-IgG1/2a (BD Pharmingen Clone: G28-5, Cat: 553881). Additionally, CD169-PE (R&D Systems, 5610P) and F4/80-APC (eBiosciences, 17-4801) were used to visualize macrophage subsets. Pictures of slides were taken with Keyence BZ-9000.

Clec4F immunofluorescence

Liver tissue samples were fixed in 4% paraformaldehyde for 5 days at room temperature and embedded in paraffin and ~2 µm tissue sections were made using a microtome. The sections were later de-paraffinized, rehydrated and boiled at 100°C with EDTA to facilitate antigen retrieval. An tigen retrieval was performed with 96°C sodium citrate buffer. Slides were washed with TBS-Tween. Primary antibody, purchased from R&D systems (1:2000), and secondary antibody, purchased from Jackson ImmunoResearch (1:250), were incubated sequentially for 1 h at RT in a humid chambers. Slides were mounted in DAPI Fluoromount-G® and kept in the dark at 4°C. Slides were imaged with a confocal Zei ss LSM 710 ConfoCor 3.

1 **RNA isolation and quantitative PCR analysis**

2 Total RNA was isolated from approximately 20 mg of liver tissue lysed in RLT buffer
3 from an RNeasy mini kit (Qiagen) using a gentleMACS™ Dissociator (Miltenyi
4 Biotec). Spectrophotometric measurement of the quality and quantity of isolated
5 RNA was done using Nanodrop (ThermoFisher). 1 µg of RNA was reverse
6 transcribed to cDNA using Quantitect Reverse Transcription Kit (Qiagen) following
7 the instructions from the manufacturer. Relative mRNA expression was analyzed in
8 duplicates on 384-well PCR plates (ThermoFisher) using FastStart Universal SYBR
9 Green Master (Rox) and the qPCR was run on 7900 HT qRT-PCR system (Applied
10 Biosystems). Relative mRNA levels were calculated through $\Delta\Delta CT$ relative
11 quantification method and the obtained values were normalized to housekeeping
12 genes albumin (for liver), β -actin and GAPDH. For HBV- or HDV-infected HepaRGs,
13 total RNA and total DNA were respectively extracted from cells with the NucleoSpin
14 RNA II kit and Nucleospin® tissue kit according to the manufacturer's (Macherey-
15 Nagel) instructions. RNA reverse transcription was performed using the Superscript
16 III RT (Life Technologies). Quantitative PCR were performed specific primers and
17 normalized to PRP housekeeping gene as previously described (29, 30). TNF α - and
18 IFN- α -treated HepaRGs, were washed once with PBS, lysed in RLT buffer (Qiagen),
19 passed through a QiaShredder column (Qiagen), and RNA was extracted using the
20 RNeasy Mini Kit (Qiagen). Reverse transcription was performed with the Quantitect
21 Reverse Transcription Kit using 500 ng total RNA and subsequent qPCR analysis
22 was done by using the FastStart Universal SYBR Green Master (Rox) (Roche).

1 Immunohistological stainings

2 Liver tissue samples were fixed in 4% paraformaldehyde for 5 days at room
3 temperature and embedded in paraffin and ~2 µm tissue sections were made using
4 a microtome. The sections were later de-paraffinized, rehydrated and boiled at
5 100°C with EDTA to facilitate antigen retrieval. IHC staining was performed with a
6 Leica automated BOND-MAX staining platform using Bond Polymer Refine Detection
7 kit (Leica, Catalog #DS9800). Staining was performed using antibodies purchased
8 from Cell Signaling for pSTAT1-pY701 (1:100 dilution), and pSTAT3 (1:100 dilution),
9 from ACRIS for STAT2 (1:500 dilution), from Novus Biologicals for MHC-II (1:500
10 dilution), from Linaris for F4/80 (1:120 dilution), and from abcam for CD68 (1:300
11 dilution).

12 pSTAT1, HNF4α and F4/80 sequential staining quantification

13 Liver tissue samples were cut sequentially and treated and stained as described
14 above. pSTAT1 positive cells were manually counted in three different view fields per
15 samples. Based on cells morphology and overlaying with HNF4α positive staining,
16 pSTAT1 positive cells were divided into two groups: pSTAT1 positive hepatocytes or
17 pSTAT1 positive non-parenchymal cells (i.e. all other positive cells except
18 hepatocytes).

19 CXCL10 and TNFα RNA in situ hybridization (ISH)

20 RNA *in situ* hybridization was performed on the liver tissues by following
21 manufacturer instructions for RNAscope 2.0 FFPE Assay kit –BROWN, purchased
22 from Advanced Cell Diagnostics. Briefly, 2 µm paraffin sections mounted on glass
23 slides were boiled at 100°C in EZprep buffer for 20 min followed by a protease

treatment at 37°C for 30 min. Probes specific to mouse CXCL10 or TNF α (Advanced Cell Diagnostics) were hybridized at 48°C for 2 h using HybEZ Hybridization oven (Advanced Cell Diagnostics) followed by a subsequent series of washing and signal amplification steps. Mouse specific probe for Ubiquitin C, a common housekeeping gene is used as a positive control along with a probe for bacterial gene dapB which served as a negative control. In the end, hybridization signals were detected by DAB staining followed by counterstaining with hematoxylin. Stained tissues were digitally scanned using Leica SCN400 scanner (Leica) and hybridization signals were analyzed at 40x magnification using DIH software (Leica).

DC maturation flow cytometry

Livers and spleens were harvested, perfused with DMEM (Gibco) in the presence of 167 μ g/ml of Liberase TM Research Grade (Roche) and 200 μ g/ml of DNase I (Roche), and incubated 30 min at 37°C. Digestion was stopped by adding DMEM containing 10% FCS (Gibco). Samples were smashed through 70 μ m filter and centrifuged for 5 min at 1500 rpm. Cells were resuspended and incubated for 10 min at 4°C in FACS buffer (PBS + 1% FCS + 5 mM EDTA) in presence of 1:50 FC block (CD16/CD32 monoclonal antibody, Ebioscience). The following antibody panel (ebioscience) was incubated 30 min at 4 °C: CD8 α -PerCP-eFluor 710, CD11c-PE-Cy7, CD80-FITC, CD86-PE, CD40-APC, MHCII-APC-eFluor 780. Cells were washed with FACS buffer and centrifuged for 5 min at 1500 rpm. Cells were resuspended in FACS buffer containing DAPI and analyzed in a BD LSRFortessa™ cytometer. Analysis was then performed on Flow-Jo™.

CXCL10 ELISA

Approximatively 30 mg of liver was disrupted using 2 mm beads in a protein buffer (100 mM TRIS pH7.4, 150 mM NaCl, 1 mM EGTA, 1 mM EDTA, 1% Triton X100, 0.5% Sodium deoxycholate, 1 mM PMSF, 1X PIC). Proteins were quantified and equal concentration of total protein lysate (5 µg/ml) was used to perform the CXCL10 ELISA following manufacture instructions (R&D).

Intracellular cytokine staining

Single-cell suspensions from the liver tissues were obtained by tissue dissection and grating through a 70 µm cell strainer (Falcon). RBC lysis was performed using BD Pharm Lyse Buffer (BD Biosciences). ~ 4x10⁶ cells were used for stimulation with LCMV gp33 peptide or a non-specific peptide at a concentration of 1 µg/ml of peptide along with Brefeldin A (Golgi-plug; 1 mg/ml). Plates were later incubated for 5 h at 37°C. Surface staining was done using CD8α and cells were fixed and permeabilized (Cytofix/Cytoperm and Perm/Wash Buffer; BD Biosciences), followed by staining with mAbs to mouse IFN-γ (eBiosciences) and CD8α (eBiosciences). Cells were fixed on ice in 2% formaldehyde (diluted from Histofix 4%; Carl Roth, Karlsruhe, Germany) for 1 h followed by fluorocytometric analysis.

Primary hepatocyte isolation

Mice were anesthetized with 120 µl ketamine and xylazine (ketamine 5%, xylazine 2 mg/ml). Livers were perfused with buffer A (10 mM EGTA 1.5 ml + 48.5 ml Hank's balanced salt solution) through the portal vein for 5 min. The vena cava was cut as soon as the perfusion was started, and the perfusion was switched to buffer B (HBSS with 10 mM Calcium & Collagenase A+D, freshly prepared) and carried out until the liver turned pale (5-8 min). The liver was later removed and placed in a 100

1 μm cell strainer in a petri dish containing William's E medium. The resulting solution
2 was passed through a 100 μm (BD Biosciences) cell strainer and collected into a 50
3 ml falcon filled with 40 ml of buffer C (William's E Medium). The cell suspension was
4 centrifuged at 50 g (450 rpm) for 2 min. The resulting pellet was washed again twice
5 in 40 ml of buffer C followed by centrifugation after discarding the supernatant. After
6 the final wash step, the pellet was re-suspended in 10 ml of buffer C and the viability
7 of isolated cells was measured using trypan blue at a 1:10 dilution. A viability rate
8 above 80% was considered appropriate for experimental usage. 0.75×10^6 cells
9 were plated onto 6-well plates in required quantities and used for the experiments.

10 **HepaRG cell culture and treatments**

11 HepaRG cells were cultured, differentiated, and infected by HBV (MOI 100) and/or
12 HDV (MOI 10) as previously described (30, 31). HBV inoculum was prepared from
13 HepAD38 (32) supernatants by polyethylene-glycol-MW-8000 (PEG8000, SIGMA)
14 precipitation (8% final) as previously described (33). Viral stocks with titers of
15 superior to 1×10^{10} vge/ml were tested to be endotoxin free. HDV inoculum was
16 prepared from transfected HuH7 cells as previously described (30). Viral stocks were
17 tested to be endotoxin free. rhPEG-IFN- α (Roferon) was purchased Roche and used
18 at 500 UI/ml. TPCA-1 and ML120B were purchased from SIGMA-Aldrich and used
19 as IKK β inhibitors in Figs. 6 B and D, Figs. S5 D and E at 1 μM and 10 μM ,
20 respectively. HBeAg and HBsAg were detected in the supernatant of HBV-infected
21 cells using the Autobio kit according to the manufacturer (Autobio Diagnostics Co.).

22 **Evaluation of deletion efficiency and specificity in LysM-Cre IFNAR^{fl/fl} and Alb- 23 Cre IFNAR^{fl/fl} mice**

KCs and hepatocytes were isolated as previously described (34, 35). Following a proteinase K digestion, genomic DNA of KCs, splenocytes and hepatocytes were precipitated O/N at 4°C using 0.3M Na-acetate and ethanol as anti-solvent, washed twice with ice-cold 70% ethanol and reconstituted in nuclease-free Water. Cre-mediated excision of the loxP flanked genomic region of IFNAR exon 10 was analyzed by PCR in LysM-Cre IFNAR^{fl/fl} and Alb-CreIFNAR^{fl/fl} and IFNAR^{fl/fl} mice. The PCR reaction was designed to detect the WT allele at 1264 bp, floxed allele at 1200 bp and the recombined allele at 430 bp with the following primers – dEx10For (5'-GGT TAA GCT CCT TGC TGC TAT CTG G-3') and dEx10Rev (5'-TTG GAG ATG CAA TCT CGT ACT CAG C-3').

Generation of differentiated HepaRG^{ΔIKKβ} KO cell line

To knock out IKKβ, sgRNAs were chosen based on high scoring and no high scoring off-targets using CHOPCHOP v2 web tool (36). These sgRNAs were inserted into pUSEPR (generous gift from Dr. Tscharaganeh, unpublished) based on methods as described elsewhere (37). Briefly, a sgRNA scaffold fragment was attached to the 5' end of a U6 promoter by using overlap extension PCR. In a subsequent PCR reaction, 20 nt sgRNAs were added to the 5' end of the sgRNA scaffold and the 3' end of the U6 promoter. BsmBI sites added upstream of the 5'sgRNA and downstream of the 3'-sgRNA were used to seamlessly clone the 5'-sgRNA-sgRNA scaffold-U6 Promoter-sgRNA-3' fragment into the vector backbone via golden gate assembly (10 U BsmBI; 400 U T4 DNA Ligase; 1 mM ATP; 1x NEBuffer 3.1; 0.03 pmol vector backbone; 0.3 pmol insert). Preparation of lentiviral particles and transduction of HepaRGs were performed based on protocols from addgene.

Differentiated WT HepaRG or differentiated HepaRG-iCas9-pUSEPR (HepaRG^{ΔIKKβ}) cells were treated with 50 ng/ml of IFN-α and 10 ng/ml of TNFα for 12 h.

Patients population

This study involved a total number of 79 female at the age of 24.7 ± 4 from the East German anti-D cohort, women infected between 1978 and 1979 by administration of prophylactic anti-D immunoglobulin contaminated with hepatitis C virus (HCV) genotype 1b from a single source. All subjects were from limited geographic area in Germany with similar socioeconomic living conditions. None of these individuals had any known other risk factors for viral hepatitis or chronic liver disease and were HIV-negative at the time point of sampling (38). This studied comprised 57 with chronic (HCV RNA positive after repeated examination) and 22 has spontaneously resolved the HCV infection (HCV RNA negative after repeated examination). Diagnosis of chronic or resolved HCV infection was determined according to established guidelines based on standard serological and clinical criteria. The study has been approved by the research and ethic committee at Bonn University and informed consent was obtained from the objects prior to inclusion into the study.

Single nucleotide polymorphism Genotyping

Subjects were genotyped using TaqMan SNP Genotyping Assays with TaqMan Universal Master Mix and QuantStudio™ 6 Flex Real-Time PCR System (ThermoFisher Scientific). Differences in contingency were assessed Chi-squared using Prism software (Graphpad Prism version 5.0a). Associations were examined by the Fisher-exact test implemented in R (version 3.1.1). Allele and genotype frequencies were analyzed and tested for consistency with Hardy–Weinberg

equilibrium using a software package designed by Strom and Wienker-TUM (<http://ihg.gsf.de/ihg/snps.html>). Genotype frequencies were compared between individuals with resolved and chronic infection using 2x2 contingency tables.

Statistical analysis

A statistical analysis of the data was performed using Prism software (Graphpad Prism version 5.0a). The standard error of the mean was calculated from the average of at least 3 independent samples in a given treatment condition. To evaluate statistical significance, obtained results were subjected to Student's t-test (unpaired, two-tailed test) and a p-value of less than 0.05 was considered significant.

* $p < 0.05$, ** $p < 0.01$, *** $p < 0.001$.

Results

LCMV-induced hepatocytic NF- κ B signaling is required for hepatic virus control, independent of Kupffer cell-derived factors.

Given the central role of NF- κ B signaling in PRR-mediated viral sensing and activation of innate immunity, we tested whether LCMV infection would activate NF- κ B signaling in liver parenchymal cells. To this end, WT mice were intravenously (i.v) infected with 2×10^6 PFU of LCMV, and 12 hours post-infection (p.i.), nuclear RelA translocation was analyzed in livers by immunohistochemistry. Notably, nuclear RelA translocation was found in hepatocytes and to a lesser degree in KCs of infected livers (**Fig. 1 A**). As TNF α is a major driver of nuclear RelA translocation, we first investigated hepatic TNF α expression. LCMV infection elevated TNF α mRNA in liver and TNF α protein in serum (**Figs. S1 A, upper and lower left panels**), which could be mainly localized to non-parenchymal cells as analyzed by RNA *in situ* hybridization (**Fig. S1 A, right panel**). Further, sequential staining of TNF α by RNA *in situ* hybridization with F4/80 demonstrated that the majority of TNF α mRNA expressing cells are F4/80⁺ Kupffer cells (**Fig. S1 B**). To determine whether Kupffer cells, the major TNF α -producing cell type in the liver or other phagocytosing antigen presenting cells (APCs) were required for LCMV-induced nuclear RelA translocation in hepatocytes, mice were treated with clodronate liposomes prior to infection, which efficiently depleted phagocytic F4/80⁺ cells in liver (**Fig. S1 C**). Despite the efficient depletion of Kupffer cells, efficacy of nuclear RelA translocation in hepatocytes remain unchanged at 24 h p.i. (**Fig. S1 C**). Moreover, TNFR1^{-/-} mice displayed unchanged nuclear RelA translocation upon LCMV infection when compared to WT livers (**Figs. S1 D and S1 E**). Consecutive staining of RelA/HNF4 α or RelA/F4/80 in

livers of TNFR1^{-/-} mice indicated that RelA translocation can be found mainly in hepatocytes (**Fig. S1 F**). This suggests that LCMV-induced RelA translocation and subsequent NF-κB signaling in hepatocytes is not mediated by phagocytic immune cell populations such as Kupffer cells or cytokines produced by the latter and could be due to the sensing of LCMV through pathogen recognition receptors (PRRs), such as TLR3 within hepatocytes (**Figs. S1 D and S1 E**).

To determine which PRRs were required for LCMV-mediated RelA translocation in hepatocytes, we infected mice lacking several key viral sensing molecules with LCMV (**Figs. S1 D and E**). Hepatocytic RelA translocation was significantly reduced in livers of Tlr3^{-/-} or Tlr7^{-/-} mice after LCMV infection, indicating that intracellular RNA sensing by these PRRs is involved. Loss of the adapter protein for RIG-I and MDA5 signaling, MAVS, and a key adapter protein in TLR signaling - MyD88 - also resulted in a significant reduction in nuclear RelA translocation in hepatocytes post-LCMV infection. In contrast, nuclear RelA levels remained unchanged in hepatocytes devoid of STING (Sting^{-/-}), an intracellular DNA sensor, compared to WT (**Figs. S1 D and E**).

To elucidate the role of hepatocyte-specific NF-κB signaling in the context of virus infections, we next analyzed mice with a selective deletion of IKKβ in liver parenchymal cells (IKKβ^{ΔHep} mice). Specific deletion of IKKβ in liver parenchymal cells was confirmed via mRNA expression analysis of whole livers, spleens for control, and isolated hepatocytes from IKKβ^{ΔHep} and WT mice (**Fig. S1 G**). WT and IKKβ^{ΔHep} mice were infected i.v. with LCMV and stained for RelA. Nuclear RelA translocation was observed in hepatocytes from LCMV-infected WT mice with a peak at 12 hours p.i., whereas IKKβ^{ΔHep} mice infected with the same dose of LCMV-WE

lacked significant RelA translocation in nuclei of hepatocytes (**Fig. 1 B**). Of note, activation of the JNK pathway, analyzed by cJUN phosphorylation and subsequent nuclear translocation, was lower in $\text{IKK}\beta^{\Delta\text{Hep}}$ mice compared to WT (**Fig. S1 H**).

To evaluate the functional consequence of hepatocyte-specific inhibition of canonical NF- κ B signaling, we compared virus titers from the livers of $\text{IKK}\beta^{\Delta\text{Hep}}$ and WT mice infected with different doses of LCMV. Strikingly, an approximately 100-fold increase in virus titers at the peak of infection was found in livers of $\text{IKK}\beta^{\Delta\text{Hep}}$ mice when compared to WT mice (**Fig. 1 C**). Similar virus titers in spleens of $\text{IKK}\beta^{\Delta\text{Hep}}$ as in WT mice suggest that peripheral virus control is not dramatically affected (**Fig. S1 I**). Furthermore, abundance of CD169⁺ splenic macrophages was analyzed in WT and $\text{IKK}\beta^{\Delta\text{Hep}}$ mice by immunofluorescence and not found to be significantly different (**Fig. S1 J**). In addition, flow cytometry of splenic and hepatic immune cells did not reveal differences in DC maturation between the WT and $\text{IKK}\beta^{\Delta\text{Hep}}$ mice at day 3 p.i. (**Fig. S1 K**).

LCMV predominantly accumulates in hepatocytes of $\text{IKK}\beta^{\Delta\text{Hep}}$ livers

To identify the cell types in which LCMV is accumulating and actively replicating over time, we analyzed the cellular localization of LCMV in frozen liver sections of WT and $\text{IKK}\beta^{\Delta\text{Hep}}$ mice post-infection with 2×10^6 PFU of LCMV at different time points by staining for LCMV nucleoprotein (NP) (24, 39). While LCMV-WE was localized to cells exhibiting Kupffer cell-like morphology as early as day 2 p.i., LCMV-WE was sporadically also detected in hepatocytes by days 6 and 8 p.i. in WT livers, indicating that LCMV-WE also replicates at very low levels in hepatocytes (**Fig. 1 D**) contrary to

earlier findings illustrating Kupffer cells as the only cell type in the liver responsible for the intake and reduction of liver virus titers (24). Strikingly, hepatocytes from $IKK\beta^{\Delta Hep}$ mice displayed large clusters filled with LCMV-NP, particularly at days 6 and 8 p.i., due to defective NF- κ B signaling in hepatocytes (**Fig. 1 D**). An approximate 10-fold increase in LCMV-WE⁺ hepatic area was found in $IKK\beta^{\Delta Hep}$ compared to WT livers (**Fig. 1 D**). Co-stains of LCMV-NP with F4/80⁺ (Kupffer cells) or HNF4 α ⁺ (hepatocytes) demonstrated that at day 2 p.i., LCMV-NP localized exclusively in macrophages, whereas at days 6 and 8 p.i., LCMV⁺ cells in $IKK\beta^{\Delta Hep}$ livers were mainly hepatocytes, as identified by positive staining for HNF4 α (**Figs. 1 E and Fig S1 L**). Of note, whereas the initial number of LCMV-infected F4/80⁺ cells was similar between both genotypes at day 2 p.i., a significantly higher number of LCMV-infected F4/80⁺ cells was observed in $IKK\beta^{\Delta Hep}$ than in WT livers at day 8 p.i. (**Fig. 1 E**).

Loss of NF- κ B signaling in hepatocytes leads to impaired IFN responses

Considering the critical role of $IKK\beta$ in the induction of IFN responses (19, 40, 41), we investigated whether $IKK\beta^{\Delta Hep}$ livers were defective in the early induction of IFN responses following LCMV infection. To this end, WT and $IKK\beta^{\Delta Hep}$ mice were infected with LCMV, and ISG expression was measured over time by qPCR. A reduction in ISG expression was observed in livers of $IKK\beta^{\Delta Hep}$ compared to WT, especially at 18 hours and 24 hours p.i. (**Fig. 2 A**). Among the differentially expressed ISGs, Mx1, IFIT1, IFIT2, OAS1, OAS3 were significantly reduced in $IKK\beta^{\Delta Hep}$ mice (**Figs. 2 A and S2 A**). Furthermore, expression of IFN-dependent

chemokines such as CXCL9, and CXCL10 important for the chemo-attraction of immune cells such as monocytes, and T cells were reduced in $\text{IKK}\beta^{\Delta\text{Hep}}$ livers due to hepatocyte-specific loss of canonical NF- κ B signaling (**Fig. 2 A**).

As CXCL10 mRNA is abundantly expressed in the liver following IFN induction, it was used as a marker to monitor antiviral IFN responses following LCMV infection by sequential CXCL10 RNA *in situ* hybridization and HNF4 α IHC in livers of WT and $\text{IKK}\beta^{\Delta\text{Hep}}$ mice (**Fig. 2 B**). RNA expression of CXCL10 was reduced in hepatocytes (HNF4 α^+ cells) of $\text{IKK}\beta^{\Delta\text{Hep}}$ livers, whereas the non-parenchymal compartment (e.g. Kupffer cells) still strongly expressed *Cxcl10* mRNA (**Fig. 2 B**). In contrast, in infected WT livers, both hepatocytes and non-parenchymal cells expressed *Cxcl10* mRNA at high levels following infection. This highlights the importance of hepatocyte-intrinsic canonical NF- κ B signaling in amplifying ISGs within hepatocytes following LCMV infection. Moreover, CXCL10 protein expression was reduced in $\text{IKK}\beta^{\Delta\text{Hep}}$ liver compared to WT liver at 18 and 24 hours (**Fig. 2 C**). We did not observe a difference in mRNA expression of IFN- α or IFN- β in WT and $\text{IKK}\beta^{\Delta\text{Hep}}$ livers, thus the observed differences in ISGs most likely derive from defective IFN amplification loops in hepatocytes lacking NF- κ B signaling (**Fig. S2 A**). We further tested this reasoning by intravenously injecting IFN- α into WT and $\text{IKK}\beta^{\Delta\text{Hep}}$ mice. Two hours later, mRNA expression of several ISGs was analyzed, which demonstrated significant reduction in $\text{IKK}\beta^{\Delta\text{Hep}}$ livers compared to WT, despite having been exposed to similar amounts of IFN- α (**Fig. 2 D**).

Signal transducer and activator of transcription 1 (STAT1) is a central transcription factor which forms heterodimers with STAT2 upon activation by type I and type III

IFNs. These heterodimers translocate into the nucleus and bind to IFN-stimulated response elements (ISREs), thereby enhancing ISG expression (42). Strong nuclear pSTAT1 staining was observed in hepatocytes (red arrow heads in **Fig. S2 B**) of LCMV-infected WT livers at 18 hours p.i., which was reduced in $\text{IKK}\beta^{\Delta\text{Hep}}$ hepatocytes. In contrast, non-parenchymal cells (black asterisks) were equally positive for pSTAT1 in both genotypes (**Fig. S2 B**). Reduction of nuclear pSTAT1 in hepatocytes is consistent with lower total STAT1 mRNA expression in whole liver tissue and in hepatocytes of $\text{IKK}\beta^{\Delta\text{Hep}}$ mice (**Figs. 3 A and B**). In contrast, neither STAT2 nor STAT3 phosphorylation (**Figs. S2 C and D**) were changed in $\text{IKK}\beta^{\Delta\text{Hep}}$ livers compared to WT. To elucidate whether the reduction of pSTAT1 was indeed specific for hepatocytes, consecutive staining of HNF4 α -pSTAT1-F4/80 liver sections derived from WT and $\text{IKK}\beta^{\Delta\text{Hep}}$ mice 18 hours p.i. was performed. These experiments and subsequent quantitative analyses indicated that in $\text{IKK}\beta^{\Delta\text{Hep}}$ livers, pSTAT1 staining is significantly reduced in HNF4 α^+ hepatocytes, but remained unchanged in F4/80 $^+$ Kupffer cells (**Fig. S2 E**). Taken together, these experiments indicate that hepatocyte-specific suppression of canonical NF- κ B signaling in $\text{IKK}\beta^{\Delta\text{Hep}}$ mice leads to reduced mRNA expression and phosphorylation of STAT1 and STAT1-dependent ISG induction without affecting pStat1 levels or selected ISGs in non-parenchymal cells.

Impaired ISG responses and impaired viral control in $\text{IKK}\beta^{\Delta\text{Hep}}$ livers are hepatocyte-intrinsic

To determine whether increased virus titers and reduced ISG expression in $\text{IKK}\beta^{\Delta\text{Hep}}$ livers were caused by an inability of $\text{IKK}\beta^{\Delta\text{Hep}}$ hepatocytes to integrate paracrine signaling from other cells (e.g. Kupffer cells) or due to an intrinsic autocrine signaling defect, hepatocytes isolated from $\text{IKK}\beta^{\Delta\text{Hep}}$ and WT livers were infected with LCMV *ex vivo* (**Fig. 3 A**). Total cell lysates were analyzed for the expression of viral transcripts and ISGs. A significant increase in expression of LCMV-NP was observed in $\text{IKK}\beta^{\Delta\text{Hep}}$ hepatocytes compared to WT, as well as a decrease in expression of several ISGs (**Fig. 3 B**).

The importance of NF- κ B signaling in amplifying ISGs was further verified by treating cultured primary hepatocytes *ex vivo* with IFN- α . $\text{IKK}\beta$ -deficient hepatocytes displayed reduced induction of ISGs compared to WT hepatocytes (**Fig. 3 C**). Furthermore, no significant differences were observed in IFN- α and IFN- β mRNA expression in *ex vivo* cultivated, LCMV-infected hepatocytes from $\text{IKK}\beta^{\Delta\text{Hep}}$ and WT at 18 hours and 24 hours p.i. (**Fig. S2 F**). Thus, hepatocyte-intrinsic canonical NF- κ B signaling is indispensable for efficient expression of ISGs.

Hepatic ISGs can be expressed in the absence of hepatic APCs or Kupffer cells

To further test the interplay between Kupffer cells and hepatocytes in the generation of hepatic immune responses, mice were treated with clodronate-containing or empty (PBS) liposomes prior to LCMV infection. Virus titers were measured in livers of both groups at 1 day p.i. An increase in virus titers from mice with clodronate depletion was found at 1 day p.i., suggesting that phagocytic immune cells such as

Kupffer cells are required for optimal control of initial viral replication in hepatocytes. **(Figs. S3 A and B)**. Despite significant differences in the mRNA expression of Mx1, OAS2, and OAS3 in the absence of myeloid cells, expression levels of IFN- β and other ISGs such as ISG15, IFIT1 and CXCL10 were not significantly changed. Thus, early after infection, several hepatic ISGs can be expressed in the absence of Kupffer cells or hepatic APCs **(Fig. S3 C)**.

LCMV accumulates in hepatocytes from mice with defective hepatocyte-specific IFN signaling

Our results so far indicated that defective NF- κ B signaling in hepatocytes dampened IFN responses in liver tissue and facilitated enhanced LCMV replication. To determine the relative contribution of liver parenchymal- or myeloid-specific IFN signaling to viral control, mice lacking IFNAR1 receptor selectively in liver parenchymal cells (IFNAR ^{Δ Hep}) (20, 26) or myeloid cells, including Kupffer cells (IFNAR ^{Δ Myel}) (26, 43) were infected with LCMV. The efficacy and specificity of IFNAR1 deletion was analyzed in hepatocytes, Kupffer cells or hepatic inflammatory myeloid cells by PCR. IFNAR was deleted with high efficacy in hepatocytes and Kupffer cells, but less so in liver-infiltrating monocytes **(Fig. S3 D)**.

Upon infection, LCMV-NP protein expression was analyzed in IFNAR ^{Δ Hep}, IFNAR ^{Δ Myel}, IKK β ^{Δ Hep}, and WT livers. Similar to IKK β ^{Δ Hep}, livers of IFNAR ^{Δ Hep} mice displayed LCMV-positive hepatocyte clusters at day 6 and 8 p.i. **(Fig. 4 A)**, supporting our hypothesis that a robust early hepatocyte-intrinsic IFN response (amplified by IKK β) through IFNAR is required for efficient ISG expression and viral

control in the liver. Notably, infected IFNAR^{ΔMyel} mice displayed impaired protection against viral replication, as both Kupffer cells and hepatocytes were strongly positive for LCMV-NP at day 6 p.i. However, the intensity of LCMV-NP expression in IFNAR^{ΔMyel} mice decreased in hepatocytes by day 8 p.i. and was primarily localized to F4/80⁺ cells (**Figs. 4 A and B**), indicating that hepatocytes respond both to paracrine IFN signaling coming from Kupffer cells and to autocrine IFN signaling from hepatocytes (**Fig. 4 B**).

Hepatocytes are the major producers of ISGs in the liver following LCMV infection

To further delineate the functional importance of hepatocyte versus myeloid cell-mediated IFN production and IFN responses, whole liver lysates from WT, IKKβ^{ΔHep}, IFNAR^{ΔHep}, and IFNAR^{ΔMyel} mice were analyzed for IFN and ISG expression up to 24 hours after LCMV infection. Overall, IFN-β mRNA expression in livers was decreased during early phases of LCMV-WE infection (12 hours p.i.) in IFNAR^{ΔMyel} livers compared to IFNAR^{ΔHep}, Ikkβ^{ΔHep}, and WT livers but not at later time points (**Fig. S3 E**). This suggests that efficient, early IFN-β expression depends on KCs and myeloid IFNAR expression. Moreover, early-induced ISGs such as ISG15, Mx1, and STAT1, as well as IFN-induced chemokines such as CXCL10 were more strongly upregulated in WT compared to IFNAR^{ΔHep} (strongest reduction), IFNAR^{ΔMyel} and Ikkβ^{ΔHep} livers at 18 hours p.i. (**Fig. 4 C**). Although ISG expression was decreased in IFNAR^{ΔMyel} compared to WT livers, the expression levels were similar to Ikkβ^{ΔHep} livers and significantly higher when compared to IFNAR^{ΔHep} (**Fig. 4 C**).

Immunohistochemical analyses revealed reduced pSTAT1 signals in hepatocyte nuclei of LCMV-infected IFNAR^{ΔHep} livers compared to WT at 12 hours and 18 hours p.i., whereas pSTAT1 in myeloid cells remained unaffected (**Fig. 4 D**). In contrast, IFNAR^{ΔMyel} livers displayed reduced pSTAT1 in both hepatocytes and myeloid cells at 12 hours p.i. (**Figs. 4 D and S3 F**), indicative of a delayed IFN response in hepatocytes due to impaired IFNAR signaling in myeloid cells. These observations were confirmed by consecutive staining of HNF4α-pSTAT1-F4/80 in livers of WT and IFNAR^{ΔMyel} mice. Our data indicate that in IFNAR^{ΔMyel} mice livers, pSTAT1 staining is strongly reduced in F4/80⁺ Kupffer cells, and significantly lowered in HNF4α⁺ hepatocytes, in comparison to WT mice (**Figs. S2 E and S3 G**). Of note, hepatocyte-specific RelA translocation occurred in WT, IFNAR^{ΔHep}, and IFNAR^{ΔMyel} with similar efficacy (**Fig. 4 E**). This indicates that having an intact NF-κB signaling, hepatocytes integrate paracrine IFNAR signaling from the neighboring KCs and initiate an antiviral response at an early stage as well as an intrinsic autocrine IFNAR signaling.

Depletion of IKKβ in hepatocytes reduces LCMV-induced chemokine expression and immune cell influx

Efficient activation of IFN signaling in hepatocytes is NF-κB-dependent and is important for cell-intrinsic control of viral replication and dissemination. IFN responses also promote cytotoxic CD8⁺ T-cell responses (44) and may inhibit or suppress regulatory CD4⁺ T-cell responses during acute LCMV infections (45). IFN and NF-κB-driven expression of CXCR3 ligand supports the infiltration of cytotoxic CD8⁺ T cells to sites of inflammation, and hepatocytes are a known source of

CXCR3 ligands such as CXCL9, CXCL10 and CXCL11 during viral infections and autoimmune disease (46-48). Since we observed an increased viral load in $IKK\beta^{\Delta Hep}$ compared to WT livers at day 6 and 8 p.i., we investigated whether alterations in chemokine expression or subsequent intrahepatic immune cell attraction could be detected.

Real time PCR analysis of LCMV-infected liver homogenates revealed reduced expression of chemokines such as CCL5, CXCL9, CXCL10 and CXCL11 at 6 and 8 days p.i., but not at 15 days p.i., in $IKK\beta^{\Delta Hep}$ mice compared to WT (**Fig. 5 A**). To determine whether intrahepatic recruitment of $CD8^+$ T cells was consequently affected, we analyzed the abundance of $CD8^+$ T cells in livers of LCMV-infected $IKK\beta^{\Delta Hep}$ and WT mice via immunohistochemistry. Densitometric analyses of images indicated significant lower numbers of $CD8^+$ T cells at days 6 and 8 p.i. in livers of $IKK\beta^{\Delta Hep}$ mice (**Fig. 5 B**). At 15 and 20 days p.i., no significant differences were observed in the abundance of $CD8^+$ T cells, highlighting similar $CD8^+$ T cell recruitment efficacy at later time points in both genotypes (**Fig. 5 C**). Moreover, FACS analysis revealed a reduction in the number of LCMV-specific $CD8^+$ T cells at day 6 p.i. in livers of $IKK\beta^{\Delta Hep}$ mice (**Fig. 5 D**).

CXCR3 ligands also initiate robust inflammatory cascades by interacting with their cognate receptor, highly expressed on immune cells such as Kupffer cells, dendritic cells, neutrophils, natural killer cells and natural killer T cells. Since we identified a decrease in hepatocyte-derived CXCL10 during both the innate (**Fig. 2 A**) and adaptive phases (**Fig. 5 A**) of the immune response against LCMV infection, we reasoned that innate immune cell infiltration and activation in livers during the early and late phases of infection could be affected in $IKK\beta^{\Delta Hep}$ mice. Interestingly, we

observed reduced mRNA expression of CCL5, CD14, iNOS, CD11b, Ly6C and CD207 during the early phase of LCMV-WE infection (**Fig. S4 A**). CCL4, CCR5 and Ly6C were further reduced in expression during the late phase (**Fig. S4 B**). Moreover, we observed a significant reduction in intrahepatic infiltration of CD68⁺ monocytes and MHCII⁺ cells, plausibly due to reduced chemokine expression during late-stage LCMV-WE infection (**Fig. S4 C**). Of note, F4/80⁺ Kupffer cells were not significantly altered in number in both genotypes (**Fig. S4 C**). These results were confirmed by stainings of liver sections using a Kupffer cell-specific marker, Clec4F (**Fig. S4 D**). Taken together, these experiments identified a dual role for hepatocyte-specific canonical NF- κ B signaling in (1) inducing an adequate cell-intrinsic early, antiviral response and (2) subsequent viral clearance by attracting adaptive and innate immune cells to the liver.

Loss of NF- κ B signaling in differentiated HepaRG cells impairs ISG expression post-treatment with IFN- α or following HBV and HDV infection

We demonstrated that ablation of IKK β specifically in hepatocytes significantly impairs an early, efficient viral response to LCMV infection in mouse livers. LCMV infection has been used as a surrogate model for hepatitis virus infection (49). To determine whether similar mechanisms operated in human cells infected with distinct viruses, we utilized differentiated HepaRG cells (dHepaRG) devoid of IKK β protein expression (HepaRG^{TR-Cas9 IKK β}) generated by CRISPR/Cas9 gene editing or WT HepaRG cells (**Figs. S5 A and B**). The requirement for IKK β in ISG induction was tested by treating with IFN- α alone or IFN- α /TNF α . Similar to primary murine

hepatocytes lacking IKK β (**Fig. 3 B**), dHepaRG-TR-Cas9 IKK β displayed significantly reduced ISG expression compared to Cas9-control dHepaRGs after exposure to IFN- α (data not shown) or IFN- α /TNF α (**Fig. 6 A**).

Hepatitis Delta Virus (HDV), a satellite virus of HBV, has been shown to strongly activate the IFN pathway in hepatocytes (30, 50, 51). We thus analyzed ISG mRNA expression upon HDV infection in the absence of NF- κ B signaling in WT HepaRG and HepaRG-TR-Cas9 IKK β . To this end, a pharmacological inhibitor of NF- κ B signaling (ML120B) was used to treat dHepaRG cells before infection with HDV. The levels of HDV-induced ISGs, such as Viperin, Mx1, OAS1, were decreased in HepaRGs treated with inhibitor (**Fig. 6 B**). Expression of the canonical NF- κ B target gene A20, which induces a negative feedback loop to block NF- κ B signaling, was slightly induced by HDV and blocked in the presence of the inhibitor (**Fig. 6 B**). Consistent with these findings, HepaRG-TR-Cas9 IKK β cells infected with HDV displayed reduced expression of ISGs (**Fig. S5 C**). Thus, NF- κ B signaling appears to effectively increase the IFN response initiated by HDV in human dHepaRG.

Current knowledge from both experimental and clinical studies suggests that hepatitis B virus is a weak inducer of innate responses (e.g. IFN and ISGs) and has evolved strategies to evade sensing (33, 52, 53). Thus, replication of HBV can be controlled by adding exogenous IFN- α . We therefore tested whether the inhibitory action of IFN- α on HBV would be dampened in the absence of NF- κ B signaling. To this end, a pharmacological inhibitor of NF- κ B signaling was used to treat HBV-infected dHepaRGs. First, dHepaRGs were treated with IKK β Inhibitor or control (DMSO) followed by IFN- α treatment alone. It has been shown that type I IFN signaling activates NF- κ B signaling in various human and murine cell types (54).

Consistently, IFN- α -induced RelA phosphorylation was reduced in the presence of the NF- κ B inhibitor, as verified by Western blot analysis of protein lysates from inhibitor or mock-treated HepaRGs (**Fig. S5 D**). Next, IKK β inhibitor or untreated dHepaRGs were infected with HBV and then treated with IFN- α (**Fig. 6 C**). IKK β inhibition effectively dampened IFN- α -mediated suppression of HBV DNA, RNA, as well as HBV antigens (HBsAg, HBeAg) (**Fig. S5 E**). Expression of ISGs such as Mx1, OAS1, and ISG15, required for controlling HBV replication, were decreased in HBV + IFN- α -treated HepaRGs in the presence of the IKK β inhibitor (**Fig. 6 D**). Moreover, expression of the canonical NF- κ B target gene, A20, was also reduced (**Fig. 6 D**). Thus, intact NF- κ B signaling appears to be required for optimal effectiveness of IFN- α treatment against HBV infection.

To further decipher the role of NF- κ B in the response to viral infection in patients, we analysed the polymorphism of NF- κ B 1 in the serum of patients chronically infected with HCV or of patients who have resolved HCV infection (**Fig. S6**). To decipher role of NF- κ B in HCV infection, we analysed 6 specific NF- κ B 1 single nucleotides polymorphisms (SNPs) – including the homozygote (SNP^{+/+}), heterozygote (SNP^{+/-}) SNP state as well as the loss of SNP (SNP^{wt/wt}) in a cohort of approximately 80 patients. Three different groups of NF- κ B 1 SNPs were identified (**Fig. S6**): (1) SNPs that are not significantly differentially represented between chronic HCV carriers and resolvers (SNP4 and SNP5); (2) Homozygote SNPs (SNP^{+/+}) (SNP1 and SNP2) that are significantly increased in chronic HCV carriers versus HCV resolvers; (3) SNP^{wt/wt} (SNP3 and SNP6) which are significantly increased in chronic HCV carriers versus HCV resolvers. Altogether, these results indicate that SNPs in NF- κ B

- 1 are correlated with clearance or chronic infection of HCV and thus may play a role in
- 2 the resolution of HCV infection.

3

Journal Pre-proof

Discussion

While hepatocytes are known to execute metabolic functions in the liver, their role in anti-bacterial innate immunity has been well established, including expression of antibacterial proteins like complement proteins, opsonins and fibrinogen (7, 55). Hepatic viral infections, such as HBV and HCV lead to chronic hepatitis, cirrhosis and hepatocellular carcinoma, causing millions of deaths worldwide (3). During such chronic viral infections, innate sensing mechanisms are antagonized by viral proteins within infected hepatocytes which would otherwise control the virus which implicates functional antiviral mechanisms within the cells. Work focused delineating the involvement of liver cell types in clearing viral infections identified KCs as the principle cell type for virus control through IFN-mediated anti-viral signaling (3). Considering that the major molecular signaling pathways involved in viral control within hepatocytes are similar to those in immune cells, we hypothesized that hepatocyte-derived innate immune signalling might play a central role in controlling hepatic viral infections.

Here, we show that hepatocyte-specific NF- κ B activation is essential for a timely and efficient hepatic viral control. Loss of NF- κ B signaling in hepatocytes resulted in a delay of the early IFN response and, consequently, in a 100-fold virus titer increase in an LCMV-WE infection model. Of particular note, this blockade of NF- κ B signaling in hepatocytes was sufficient to enhance virus replication despite the presence of intact overall hepatic IFN- α signaling in hepatocytes and fully functional Kupffer cells. The absence of LCMV in KCs from WT livers and its presence in KCs from IKK $\beta^{\Delta\text{Hep}}$ livers at day 8 p.i. - at a time point at which a robust adaptive immune response is activated - suggests that Kupffer cell-derived signaling alone (IFN, NF- κ B) does not

1 suffice to suppress viral growth in the liver when NF- κ B signaling is inhibited in
2 hepatocytes.

3 Initially, we considered the possibility that Kupffer cell- or other APC-derived signals
4 might be required for LCMV-induced nuclear RelA translocation in hepatocytes,
5 since Kupffer cells are known to be major producers of molecules that stimulate NF-
6 κ B signaling, including TNF α . However, nuclear RelA translocation in hepatocytes
7 after LCMV-WE infection persisted even when Kupffer cells were depleted or when
8 TNFR1 was knocked out. This indicated that nuclear RelA translocation was
9 independent of molecular cues/cytokines derived from Kupffer cells/APCs, the TNF-
10 TNFR1-axis and could be a result of direct sensing of LCMV by PRRs within the
11 hepatocytes, as highlighted by the decrease of RelA translocation upon TLR3, TLR7,
12 MyD88, or MAVS knock down. For control, Sting^{-/-} mice, did not display a decrease
13 in RelA translocation.

14 Mice with hepatocyte-specific deletion of IKK β (IKK $\beta^{\Delta\text{Hep}}$) and consequently defective
15 RelA translocation showed increased virus replication and delayed virus clearance.
16 Thus, induction of RelA in hepatocytes contributes to efficient virus control in liver.
17 Notably, in livers of IKK $\beta^{\Delta\text{Hep}}$ mice, IFN-induced mRNA expression of ISGs and
18 consequent phosphorylation of STAT1 was found to be delayed and reduced in the
19 hepatocytic compartment, whereas it was still immuno-positive in the non-
20 parenchymal cell compartment compared to the livers of WT mice in which both
21 hepatocytes and non-parenchymal cells exhibited equal levels of pSTAT1.
22 Interestingly, this happened in the context of unchanged IFN- α /IFN- β expression
23 levels in IKK $\beta^{\Delta\text{Hep}}$ mice. We next found that livers depleted of KCs by clodronate also
24 expressed IFN- β levels similar to WT, whereas some ISGs were expressed at lower

1 levels in clodronate-treated livers. The residual IFN- β expression in KC-depleted
2 livers could plausibly be derived from other immune cells. Our experiments indicated
3 that myeloid cells expressing IFNAR are important for inducing the early expression
4 of ISGs and hepatocytic pSTAT1. Interestingly, reduced IFN- β expression and a
5 delay in pSTAT1 translocation in hepatocytes in IFNAR $^{\Delta Myel}$ livers indicate that
6 hepatocytes might require initial IFN cues from KCs. Accordingly, during the effector
7 phase of infection at day 6 p.i., there was a massive accumulation of LCMV in both
8 KCs and hepatocytes in IFNAR $^{\Delta Myel}$ livers. Remarkably, by day 8 p.i. there was a
9 strong decrease in the number of infected hepatocytes, whereas LCMV levels in
10 myeloid cells remained high. This indicated that hepatocyte-specific ISG expression
11 and viral control within hepatocytes, eventually occurred despite the lack of IFN
12 signaling or viral control in KCs - either due to autocrine antiviral signaling within
13 hepatocytes and/or paracrine signals from other cells (e.g. pDCs).

14 In addition, our work underlines that the hepatic increase of LCMV found in IKK $\beta^{\Delta Hep}$
15 mice is independent of LCMV-induced splenic responses, as similar levels of splenic
16 CD169 $^{+}$ macrophages and splenic DC maturation were found in WT and IKK $\beta^{\Delta Hep}$
17 mice. This finding highlights that the increased viral replication in IKK $\beta^{\Delta Hep}$ livers is a
18 causal effect of a diminished hepatocyte intrinsic innate immune response.

19 It is well established that canonical NF- κ B subunits (p50:p65) are part of an
20 enhanceosome complex along with ATF-2/c-Jun, IRF-3/IRF-7 that activates
21 Interferon- β gene expression. Also, it is known that NF- κ B activation is required for
22 the induction of pro-inflammatory cytokines, as well as early expression of IFN- β
23 during RNA virus infection and to maintain a basal level of IFN and interferon-

inducible genes (56-59). Since NF- κ B and antiviral signaling mechanisms exist in hepatocytes which constitute approximately 80% of the entire liver mass, we hypothesized that defective NF- κ B within hepatocytes would blunt the overall antiviral response in the liver. Consistent with this hypothesis, we could successfully demonstrate a direct link between the requirement of hepatocyte-intrinsic NF- κ B signaling and IFN- α responses by treating hepatocytes lacking IKK β with IFN- α directly *in vitro* and *in vivo*. In both cases, ISG expression was decreased significantly in the absence of IKK β . We could also corroborate these observations in HDV infection models or with IFN- α + TNF α treatment of dHepaRGs, where we saw blunted expression of ISGs in dHepaRGs lacking NF- κ B signaling (57, 58).

Consistent with our data, mice with hepatocyte-specific deletion of IFNAR displayed strongly reduced ISG expression and strongly increased LCMV in hepatocytes as early as 6 days p.i. Thus, presence of both IFNAR and NF- κ B signaling in hepatocytes is needed to execute optimal and timely ISG responses and control hepatic viral LCMV-infection - with IKK β and NF- κ B signaling serving as amplifiers of IFNAR signaling. Moreover, these data point to hepatocytes being an important producer of ISGs through IFNAR signaling.

Of note, expression of IFN-induced chemokines such as CXCL9, CXCL10 and CXCL11, important for the attraction of monocytes and other immune cells (60-62), were also reduced in the livers of IKK $\beta^{\Delta\text{Hep}}$ mice compared to WT. This decrease was accompanied by a reduction in the number of effector CD8 $^{+}$ T cells in IKK $\beta^{\Delta\text{Hep}}$ livers at early time points (day 6 and 8 p.i.) following LCMV infection. Notably, once LCMV infection has been controlled in both models at late time points (later than/around 15 days p.i.), no differences in hepatic CD8 $^{+}$ T cell numbers could be

1 detected. We also saw a reduction in the intrahepatic influx of innate immune cells in
2 $IKK\beta^{\Delta Hep}$ mice. Thus, in addition to impaired hepatocyte-intrinsic viral control, loss of
3 NF- κ B signaling in hepatocytes also prevents the liver from mounting an optimal
4 innate and adaptive immune response, which may further promote viral
5 accumulation and may at least partially account for the observed increase in the
6 number of LCMV-positive Kupffer cells identified in $IKK\beta^{\Delta Hep}$ livers in the current
7 study (63, 64). However, at later time points (between days 8 and 20 p.i.), LCMV-WE
8 infection was controlled - even in the absence of NF- κ B signaling in hepatocytes.

9 LCMV-WE can infect and replicate in both Kupffer cells and hepatocytes, triggering
10 potent innate and adaptive immune responses. In the case of Kupffer cell infection –
11 innate immune responses can support viral elimination, although with a delay - even
12 in the absence of hepatocytic NF- κ B. However, other hepatic viruses' which
13 specifically target hepatocytes, such as HBV or HDV, might not trigger immune
14 responses in Kupffer cells in the absence of NF- κ B signaling in hepatocytes,
15 preventing the elimination of the infection.

16 Recently, a correlation was indeed demonstrated between NF- κ B single nucleotide
17 polymorphism and susceptibility to HCV infection in different Chinese populations,
18 highlighting a role of NF- κ B in the control of hepatic viral infection (65, 66).

19 We analyzed the expression of 6 SNP of NF- κ B 1 in the serum of approximately 80
20 HCV chronically infected or resolved patients. These results confirmed the previously
21 published data (65, 66), emphasizing a possible role of NF- κ B in the activation of
22 innate immune responses (such as IFN production and signalling) and in the
23 control/resolution of hepatic viral infection.

Moreover, we showed that NF- κ B signaling is required for viral control in hepatocytes in human cells (dHepaRG) and for another virus (HDV). HBV usually does not induce strong IFN responses (67). Thus, administration of IFN- α is common therapeutic strategy for the treatment of this disease. In the current study, we demonstrated that NF- κ B signaling is required for the therapeutic effects of IFN- α treatment in the context of an HBV infection. Thus, NF- κ B signaling in hepatocytes may play a broad role in the pathogenesis of liver viral infections, as well as the molecular mechanisms underlying the efficacy of some anti-viral therapies.

In summary, we conclude that infected hepatocytes in the liver actively sense viral replication and initiate/incorporate autocrine and paracrine IFN signaling cascades and contribute to the overall production of cytokines, chemokines and ISGs. When NF- κ B signaling is impaired in hepatocytes, ISGs responses in the liver becomes markedly delayed and reduced, virus accumulates within hepatocytes, and the usually well-orchestrated adaptive immune responses during the effector phase of the infection are less effective and delayed. Thus, we propose a model of hepatic LCMV infection that can be divided in distinct phases: In the first “wave”, LCMV infects macrophages, which is associated with a strong innate immune response in these cells (e.g. TNF α). This first wave primes the upcoming wave through the secretion of IFNs, inducing the first ISGs within the liver (e.g. in Kupffer cells and other innate immune cells). In the second “wave”, LCMV is sensed by hepatocytes, preventing the establishment of the virus in cells with functional NF- κ B signaling and potent PRR responses. Taken together, our results highlight the ~~previously unrecognized~~ role played by hepatocyte-derived NF- κ B in supporting IFN-mediated immune responses and early resistance to hepatic viral infections.

1

2

3 **Acknowledgments**

4 We thank Ruth Hillermann, Danijela Heide, Olga Seelbach, Sandra Prokosch,
5 Rebecca Balduf and Jenny Hetzer for their excellent technical support.

6

7

8

Journal Pre-proof

References

1. Macpherson AJ, Heikenwalder M, Ganai-Vonarburg SC. The Liver at the Nexus of Host-Microbial Interactions. *Cell Host Microbe* 2016;20:561-571.
2. Huang LR, Wohlleber D, Reisinger F, Jenne CN, Cheng RL, Abdullah Z, Schildberg FA, et al. Intrahepatic myeloid-cell aggregates enable local proliferation of CD8(+) T cells and successful immunotherapy against chronic viral liver infection. *Nat Immunol* 2013;14:574-583.
3. Ringelhan M, Pfister D, O'Connor T, Pikarsky E, Heikenwalder M. The immunology of hepatocellular carcinoma. *Nat Immunol* 2018;19:222-232.
4. Ebe Y, Hasegawa G, Takatsuka H, Umezu H, Mitsuyama M, Arakawa M, Mukaida N, et al. The role of Kupffer cells and regulation of neutrophil migration into the liver by macrophage inflammatory protein-2 in primary listeriosis in mice. *Pathol Int* 1999;49:519-532.
5. Lee WY, Moriarty TJ, Wong CH, Zhou H, Strieter RM, van Rooijen N, Chaconas G, et al. An intravascular immune response to *Borrelia burgdorferi* involves Kupffer cells and iNKT cells. *Nat Immunol* 2010;11:295-302.
6. Crispe IN. Hepatocytes as Immunological Agents. *J Immunol* 2016;196:17-21.
7. Zhou Z, Xu MJ, Gao B. Hepatocytes: a key cell type for innate immunity. *Cell Mol Immunol* 2016;13:301-315.
8. Faure-Dupuy S, Vegna S, Aillot L, Dimier L, Esser K, Broxtermann M, Bonnin M, et al. Characterization of Pattern Recognition Receptor Expression and Functionality in Liver Primary Cells and Derived Cell Lines. *J Innate Immun* 2018:1-10.
9. Zhang X, Meng Z, Qiu S, Xu Y, Yang D, Schlaak JF, Roggendorf M, et al. Lipopolysaccharide-induced innate immune responses in primary hepatocytes downregulates woodchuck hepatitis virus replication via interferon-independent pathways. *Cell Microbiol* 2009;11:1624-1637.
10. Schneider WM, Chevillotte MD, Rice CM. Interferon-stimulated genes: a complex web of host defenses. *Annu Rev Immunol* 2014;32:513-545.
11. Lee KJ, Novella IS, Teng MN, Oldstone MB, de La Torre JC. NP and L proteins of lymphocytic choriomeningitis virus (LCMV) are sufficient for efficient transcription and replication of LCMV genomic RNA analogs. *J Virol* 2000;74:3470-3477.
12. Buchmeier MJ, Welsh RM, Dutko FJ, Oldstone MB. The virology and immunobiology of lymphocytic choriomeningitis virus infection. *Adv Immunol* 1980;30:275-331.
13. Pichlmair A, Schulz O, Tan CP, Naslund TI, Liljestrom P, Weber F, Reis e Sousa C. RIG-I-mediated antiviral responses to single-stranded RNA bearing 5'-phosphates. *Science* 2006;314:997-1001.
14. Marq JB, Hausmann S, Veillard N, Kolakofsky D, Garcin D. Short double-stranded RNAs with an overhanging 5' ppp-nucleotide, as found in arenavirus genomes, act as RIG-I decoys. *J Biol Chem* 2011;286:6108-6116.
15. Karin M, Ben-Neriah Y. Phosphorylation meets ubiquitination: the control of NF-[kappa]B activity. *Annu Rev Immunol* 2000;18:621-663.
16. Pasparakis M. Regulation of tissue homeostasis by NF-kappaB signalling: implications for inflammatory diseases. *Nat Rev Immunol* 2009;9:778-788.
17. Hiscott J, Kwon H, Genin P. Hostile takeovers: viral appropriation of the NF-kappaB pathway. *J Clin Invest* 2001;107:143-151.
18. Mohamed MR, McFadden G. NFkB inhibitors: strategies from poxviruses. *Cell Cycle* 2009;8:3125-3132.
19. Chu WM, Ostertag D, Li ZW, Chang L, Chen Y, Hu Y, Williams B, et al. JNK2 and IKKbeta are required for activating the innate response to viral infection. *Immunity* 1999;11:721-731.

20. Postic C, Shiota M, Niswender KD, Jetton TL, Chen Y, Moates JM, Shelton KD, et al. Dual roles for glucokinase in glucose homeostasis as determined by liver and pancreatic beta cell-specific gene knock-outs using Cre recombinase. *J Biol Chem* 1999;274:305-315.
21. Maeda S, Chang L, Li ZW, Luo JL, Leffert H, Karin M. IKKbeta is required for prevention of apoptosis mediated by cell-bound but not by circulating TNFalpha. *Immunity* 2003;19:725-737.
22. Park JM, Greten FR, Li ZW, Karin M. Macrophage apoptosis by anthrax lethal factor through p38 MAP kinase inhibition. *Science* 2002;297:2048-2051.
23. Maeda S, Kamata H, Luo JL, Leffert H, Karin M. IKKbeta couples hepatocyte death to cytokine-driven compensatory proliferation that promotes chemical hepatocarcinogenesis. *Cell* 2005;121:977-990.
24. Lang PA, Recher M, Honke N, Scheu S, Borkens S, Gailus N, Krings C, et al. Tissue macrophages suppress viral replication and prevent severe immunopathology in an interferon-I-dependent manner in mice. *Hepatology* 2010;52:25-32.
25. Lukashevich IS, Rodas JD, Tikhonov, II, Zapata JC, Yang Y, Djavani M, Salvato MS. LCMV-mediated hepatitis in rhesus macaques: WE but not ARM strain activates hepatocytes and induces liver regeneration. *Arch Virol* 2004;149:2319-2336.
26. Kamphuis E, Junt T, Waibler Z, Forster R, Kalinke U. Type I interferons directly regulate lymphocyte recirculation and cause transient blood lymphopenia. *Blood* 2006;108:3253-3261.
27. Yuan D HS, Berger E, Liu L, Gross N, Heinzmann F, Ringelhan M, et al. Kupffer Cell-Derived Tnf Triggers Cholangiocellular Tumorigenesis through JNK due to Chronic Mitochondrial Dysfunction and ROS. *Cancer Cell* 2017;31.
28. Honke N SN, Cadeddu G, Sorg U R, Zhang D-E, Trilling M, Klingel K, et al. Enforced viral replication activates adaptive immunity and is essential for the control of a cytopathic virus. *nature immunology* 2011;13:51-57.
29. Lucifora J, Xia Y, Reisinger F, Zhang K, Stadler D, Cheng X, Sprinzl MF, et al. Specific and nonhepatotoxic degradation of nuclear hepatitis B virus cccDNA. *Science* 2014;343:1221-1228.
30. Alfaiate D, Lucifora J, Abeywickrama-Samarakoon N, Michelet M, Testoni B, Cortay JC, Sureau C, et al. HDV RNA replication is associated with HBV repression and interferon-stimulated genes induction in super-infected hepatocytes. *Antiviral Res* 2016;136:19-31.
31. Gripon P, Rumin S, Urban S, Le Seyec J, Glaize D, Cannie I, Guyomard C, et al. Infection of a human hepatoma cell line by hepatitis B virus. *Proc Natl Acad Sci U S A* 2002;99:15655-15660.
32. Ladner SK, Otto MJ, Barker CS, Zaifert K, Wang GH, Guo JT, Seeger C, et al. Inducible expression of human hepatitis B virus (HBV) in stably transfected hepatoblastoma cells: a novel system for screening potential inhibitors of HBV replication. *Antimicrob Agents Chemother* 1997;41:1715-1720.
33. Luangsay S, Gruffaz M, Isorce N, Testoni B, Michelet M, Faure-Dupuy S, Maadadi S, et al. Early inhibition of hepatocyte innate responses by hepatitis B virus. *J Hepatol* 2015;63:1314-1322.
34. Borst K, Frenz T, Spanier J, Tegtmeyer PK, Chhatbar C, Skerra J, Ghita L, et al. Type I interferon receptor signaling delays Kupffer cell replenishment during acute fulminant viral hepatitis. *J Hepatol* 2017.
35. Abram CL, Roberge GL, Hu Y, Lowell CA. Comparative analysis of the efficiency and specificity of myeloid-Cre deleting strains using ROSA-EYFP reporter mice. *J Immunol Methods* 2014;408:89-100.
36. Labun K, Montague TG, Gagnon JA, Thyme SB, Valen E. CHOPCHOP v2: a web tool for the next generation of CRISPR genome engineering. *Nucleic Acids Res* 2016;44:W272-276.
37. Cao J, Wu L, Zhang SM, Lu M, Cheung WK, Cai W, Gale M, et al. An easy and efficient inducible CRISPR/Cas9 platform with improved specificity for multiple gene targeting. *Nucleic Acids Res* 2016;44:e149.

38. M Wiese FB, M Lafrenz, H Porst, U Oesen. Low Frequency of Cirrhosis in a Hepatitis C (Genotype 1b) Single-Source Outbreak in Germany: A 20-Year Multicenter Study. *Hepatology* 2000;32:91-96.
39. Pinschewer DD, Perez M, de la Torre JC. Role of the virus nucleoprotein in the regulation of lymphocytic choriomeningitis virus transcription and RNA replication. *J Virol* 2003;77:3882-3887.
40. Bose S, Kar N, Maitra R, DiDonato JA, Banerjee AK. Temporal activation of NF-kappaB regulates an interferon-independent innate antiviral response against cytoplasmic RNA viruses. *Proc Natl Acad Sci U S A* 2003;100:10890-10895.
41. Pauls E, Shpiro N, Pegg M, Young ER, Sorcek RJ, Tan L, Choi HG, et al. Essential role for IKKbeta in production of type 1 interferons by plasmacytoid dendritic cells. *J Biol Chem* 2012;287:19216-19228.
42. Sadler AJ, Williams BR. Interferon-inducible antiviral effectors. *Nat Rev Immunol* 2008;8:559-568.
43. Clausen BE, Burkhardt C, Reith W, Renkawitz R, Forster I. Conditional gene targeting in macrophages and granulocytes using LysMcre mice. *Transgenic Res* 1999;8:265-277.
44. Garcia-Sastre A, Biron CA. Type 1 interferons and the virus-host relationship: a lesson in detente. *Science* 2006;312:879-882.
45. Srivastava S, Koch MA, Pepper M, Campbell DJ. Type I interferons directly inhibit regulatory T cells to allow optimal antiviral T cell responses during acute LCMV infection. *J Exp Med* 2014;211:961-974.
46. Groom JR, Luster AD. CXCR3 in T cell function. *Exp Cell Res* 2011;317:620-631.
47. Harvey CE, Post JJ, Palladinetti P, Freeman AJ, Ffrench RA, Kumar RK, Marinos G, et al. Expression of the chemokine IP-10 (CXCL10) by hepatocytes in chronic hepatitis C virus infection correlates with histological severity and lobular inflammation. *J Leukoc Biol* 2003;74:360-369.
48. Nishioji K, Okanoue T, Itoh Y, Narumi S, Sakamoto M, Nakamura H, Morita A, et al. Increase of chemokine interferon-inducible protein-10 (IP-10) in the serum of patients with autoimmune liver diseases and increase of its mRNA expression in hepatocytes. *Clin Exp Immunol* 2001;123:271-279.
49. Lang PA, Contaldo C, Georgiev P, El-Badry AM, Recher M, Kurrer M, Cervantes-Barragan L, et al. Aggravation of viral hepatitis by platelet-derived serotonin. *Nat Med* 2008;14:756-761.
50. Williams V, Brichler S, Radjef N, Lebon P, Goffard A, Hober D, Fagard R, et al. Hepatitis delta virus proteins repress hepatitis B virus enhancers and activate the alpha/beta interferon-inducible MxA gene. *J Gen Virol* 2009;90:2759-2767.
51. Giersch K, Helbig M, Volz T, Allweiss L, Mancke LV, Lohse AW, Polywka S, et al. Persistent hepatitis D virus mono-infection in humanized mice is efficiently converted by hepatitis B virus to a productive co-infection. *J Hepatol* 2014;60:538-544.
52. Wieland S, Thimme R, Purcell RH, Chisari FV. Genomic analysis of the host response to hepatitis B virus infection. *Proc Natl Acad Sci U S A* 2004;101:6669-6674.
53. Dunn C, Peppas D, Khanna P, Nebbia G, Jones M, Brendish N, Lascar RM, et al. Temporal analysis of early immune responses in patients with acute hepatitis B virus infection. *Gastroenterology* 2009;137:1289-1300.
54. Yang CH, Murti A, Pfeffer SR, Basu L, Kim JG, Pfeffer LM. IFNalpha/beta promotes cell survival by activating NF-kappa B. *Proc Natl Acad Sci U S A* 2000;97:13631-13636.
55. Volanakis JE. Transcriptional regulation of complement genes. *Annu Rev Immunol* 1995;13:277-305.
56. Panne D, Maniatis T, Harrison SC. An atomic model of the interferon-beta enhanceosome. *Cell* 2007;129:1111-1123.
57. Wang J, Basagoudanavar SH, Wang X, Hopewell E, Albrecht R, Garcia-Sastre A, Balachandran S, et al. NF-kappa B RelA subunit is crucial for early IFN-beta expression and resistance to RNA virus replication. *J Immunol* 2010;185:1720-1729.

58. Basagoudanavar SH, Thapa RJ, Nogusa S, Wang J, Beg AA, Balachandran S. Distinct roles for the NF-kappa B RelA subunit during antiviral innate immune responses. *J Virol* 2011;85:2599-2610.
59. Rubio D, Xu RH, Remakus S, Krouse TE, Truckenmiller ME, Thapa RJ, Balachandran S, et al. Crosstalk between the type 1 interferon and nuclear factor kappa B pathways confers resistance to a lethal virus infection. *Cell Host Microbe* 2013;13:701-710.
60. Dufour JH, Dziejman M, Liu MT, Leung JH, Lane TE, Luster AD. IFN-gamma-inducible protein 10 (IP-10; CXCL10)-deficient mice reveal a role for IP-10 in effector T cell generation and trafficking. *J Immunol* 2002;168:3195-3204.
61. Khan IA, MacLean JA, Lee FS, Casciotti L, DeHaan E, Schwartzman JD, Luster AD. IP-10 is critical for effector T cell trafficking and host survival in *Toxoplasma gondii* infection. *Immunity* 2000;12:483-494.
62. Liu MT, Chen BP, Oertel P, Buchmeier MJ, Armstrong D, Hamilton TA, Lane TE. The T cell chemoattractant IFN-inducible protein 10 is essential in host defense against viral-induced neurologic disease. *J Immunol* 2000;165:2327-2330.
63. Wilson EB, Yamada DH, Elsaesser H, Herskovitz J, Deng J, Cheng G, Aronow BJ, et al. Blockade of chronic type I interferon signaling to control persistent LCMV infection. *Science* 2013;340:202-207.
64. Teijaro JR, Ng C, Lee AM, Sullivan BM, Sheehan KC, Welch M, Schreiber RD, et al. Persistent LCMV infection is controlled by blockade of type I interferon signaling. *Science* 2013;340:207-211.
65. Fan H Z HP, Shao J G, Tian T, Li J, Zang F, Liu M, et al. Genetic variation on the NFKB1 genes associates with the outcomes of HCV infection among Chinese Han population. *Infect Genet Evol* 2018;65:210-215.
66. Tian T WJ, Huang P, Li J, Yu R, Fan H, Xia X, et al. Genetic variations in NF-kB were associated with the susceptibility to hepatitis C virus infection among Chinese high-risk population. *Sci Rep* 2018;8(1):104.
67. Mutz P, Metz P, Lempp FA, Bender S, Qu B, Schoneweis K, Seitz S, et al. HBV Bypasses the Innate Immune Response and Does Not Protect HCV From Antiviral Activity of Interferon. *Gastroenterology* 2018.

Figure legends

Figure 1. LCMV-induced hepatocytic NF- κ B signaling is required for overall hepatic virus control independent of Kupffer cell derived factors. (A) C57BL/6 (WT) mice were intravenously (i.v.) infected with 2×10^6 PFU of LCMV-WE. 24 h post infection (p.i.), livers were harvested and frozen sections were stained for RelA (green), mainly localized in nuclei of hepatocytes (DAPI; blue; n=4). Kupffer cells (red) were stained using an anti-F4/80 antibody. RelA⁺ Hepatocytes are indicated by white arrow heads. RelA⁺ KCs are denoted by white asterisks. **(B)** C57BL/6 and IKK $\beta^{\Delta\text{Hep}}$ mice were infected i.v. with 2×10^6 PFU of LCMV-WE (n=3). Livers were isolated starting from 3 h until 24 h p.i and frozen liver sections of infected mice were stained for RelA (green) and DAPI (blue) to stain nuclei. Representative images from 12 h p.i. are shown. Livers of uninfected WT mice were used as controls. Percentage of RelA⁺ area is quantified (right panel). **(C)** WT and IKK $\beta^{\Delta\text{Hep}}$ mice were i.v. infected with 1×10^5 PFU or 2×10^5 PFU of LCMV-WE (n=3-4 for each time point). Hrs = Hours. Livers from infected mice were harvested at indicated time points and analyzed for infectious virus using a virus plaque forming assay (n=3-5 per liver tissue sample). Virus titers were normalized to mg of liver tissue. **(D) (E)** WT and IKK $\beta^{\Delta\text{Hep}}$ mice were infected i.v. with 2×10^6 PFU of LCMV-WE (n=4). Livers were isolated at different time points post infection. Frozen liver sections from infected mice were stained for LCMV-NP (green) and F4/80 (red). Co-localization signal is indicated in yellow. Representative images from indicated time points are shown. Yellow asterisks indicate non-parenchymal liver cells (e.g. Kupffer cells) positive for LCMV-NP. Error bars indicate mean \pm SEM, *p \leq 0.05, **p \leq 0.01, ***p \leq 0.001; unpaired Student's t-test.

Figure 2. Loss of NF- κ B signaling in hepatocytes leads to impaired interferon responses. WT, and IKK $\beta^{\Delta\text{Hep}}$, mice were i.v. infected with 2×10^6 PFU of LCMV-WE and a time course was performed from 0 – 24 h (n=3-4 per each time point). **(A)** Livers were isolated at indicated time points and analyzed for ISG expression through qRT-PCR. **(B)** *Cxcl10* (IP10) mRNA expression from LCMV-WE infected livers analyzed by in situ hybridization and HNF4 α staining was performed on consecutive slides. Red triangle: hepatocytes. Black asterisks: non-parenchymal cells (e.g. Kupffer cells). **(C)** CXCL10 protein was analyzed by ELISA on total liver extract and is presented as average quantity of CXCL10 per μg of total protein. **(D)** WT and IKK $\beta^{\Delta\text{Hep}}$ mice were given 500 U of IFN- α i.v. (n=3), compared to untreated WT livers and tested for the expression of ISGs through qRT-PCR. Error bars indicate mean \pm SEM, * $p \leq 0.05$, ** $p \leq 0.01$, *** $p \leq 0.001$; unpaired Student's t-test.

Figure 3. Impaired ISG responses and viral control in IKK $\beta^{\Delta\text{Hep}}$ livers is hepatocyte-intrinsic. **(A)** Schematic model describing the experiment. Hepatocytes were isolated from livers of WT and IKK $\beta^{\Delta\text{Hep}}$ mice and infected *ex vivo* with LCMV-WE (MOI=1). **(B)** RNA was extracted at the indicated time points from isolated hepatocytes and analyzed for LCMV nuclear protein (NP), glycoprotein (GP) and ISG expression. **(C)** Hepatocytes were isolated from WT and IKK $\beta^{\Delta\text{Hep}}$ mice and treated *ex vivo* with 250 U of IFN- α . RNA was extracted from hepatocytes at 12h post treatment and analyzed for the expression of ISGs. Error bars indicate mean \pm SEM, * $p \leq 0.05$, ** $p \leq 0.01$, *** $p \leq 0.001$; unpaired Student's t-test.

Figure 4. LCMV accumulates in hepatocytes from mice with defective hepatocyte-specific interferon signaling. WT, IKK $\beta^{\Delta\text{Hep}}$, IFNAR ΔHep and

IFNAR^{ΔMyel} mice were i.v. infected with 2×10^6 PFU of LCMV-WE and tested for the distribution of LCMV-NP expression (n=3-4, each time point). **(A)** Livers were isolated at the indicated time points, and stained for LCMV-NP. Representative images are shown. White asterisks: non-parenchymal liver cells LCMV-NP⁺. White arrow heads: hepatocytes LCMV-NP⁺. **(B)** Livers of infected mice of the indicated genotypes were stained with F4/80 (red), LCMV-NP (green), DAPI (blue). White arrow heads: hepatocytes. Yellow asterisks: Kupffer cells. **(C)** Livers were isolated at indicated time points and analyzed for ISG expression through qRT-PCR. **(D, E)** Histological analysis of the indicated genotypes for nuclear translocation of pSTAT1 or RelA at 12 h and 18 h p.i. Red arrow heads: hepatocytes. Black asterisks: non-parenchymal liver cells. Error bars indicate mean \pm SEM, *p \leq 0.05, **p \leq 0.01, ***p \leq 0.001; unpaired Student's t-test.

Figure 5. Depletion of IKK β in hepatocytes reduces hepatic immune cell influx and adaptive immune responses.

WT and IKK β ^{ΔHep} mice were infected i.v. with 2×10^6 PFU of LCMV-WE (n=6 each time point) and analyzed. **(A)** Livers were analyzed for the expression of selected chemokines by qRT-PCR. **(B)** Frozen liver sections were stained for CD8⁺ T cells (red), LCMV-NP (green), and F4/80 (blue). **(C)** Paraffin-embed liver sections were stained by IHC for CD8⁺ T cells. **(B, C)** Representative images from indicated time points are shown. Total CD8⁺ area was densitometrically quantified for each genotype. **(D)** Flow cytometry analysis of IFN- γ ⁺ CD8⁺ T cells isolated from the livers of LCMV infected WT and IKK β ^{ΔHep} mice 6 days p.i. and stimulated with LCMV gp33

peptide or control peptide (n = 6 each genotype). Error bars indicate mean \pm SEM, *p \leq 0.05, **p \leq 0.01, ***p \leq 0.001; unpaired Student's t-test.

Figure 6. HepaRG cells devoid of canonical NF- κ B signaling exhibit reduced expression of ISGs.

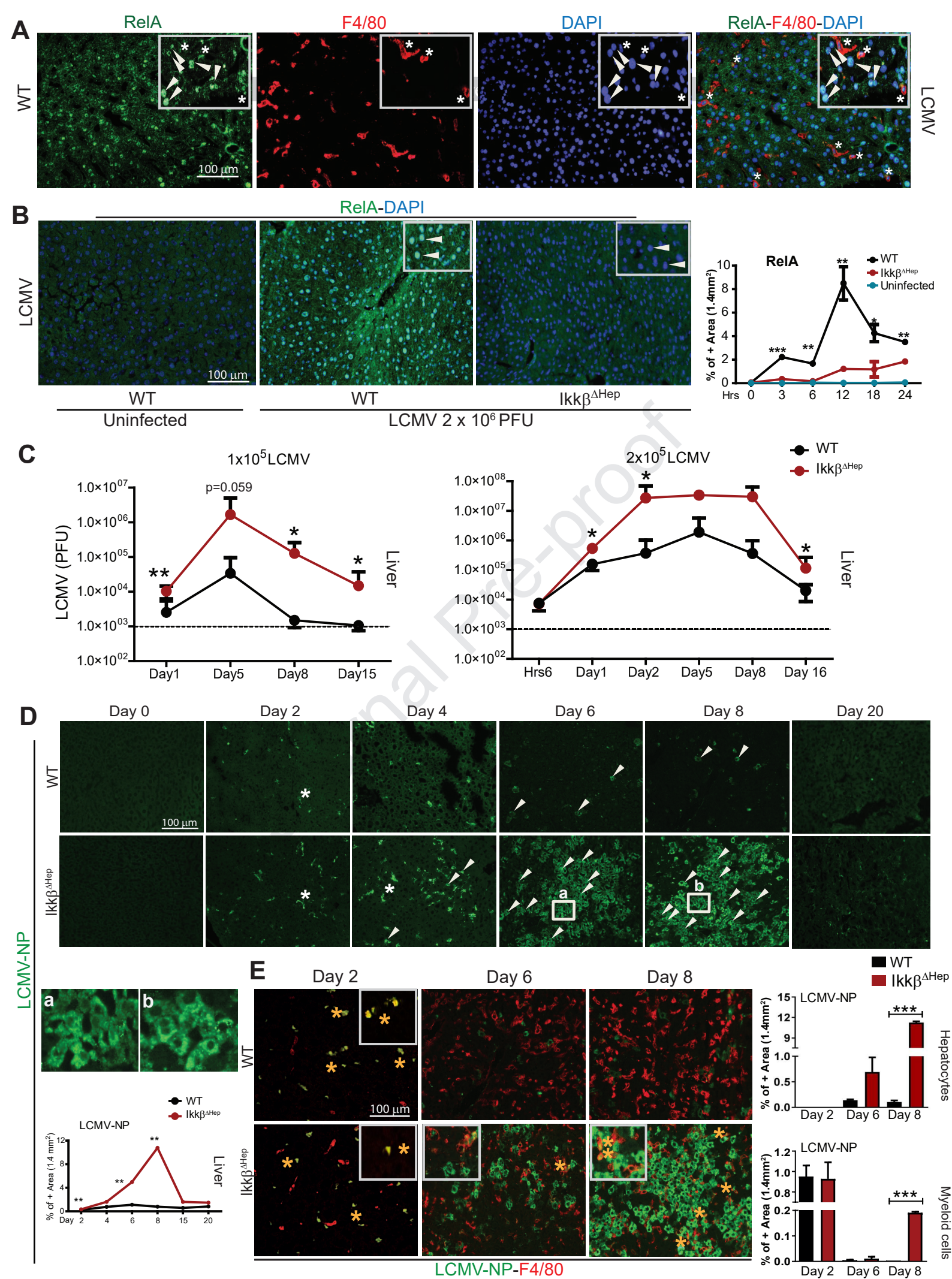
(A) HepaRGs lacking IKK β (HepaRG-TR-Cas9 IKK β) and control HepaRGs (HepaRG-TR-Cas9 CTRL) were treated for 2 h with a combination of IFN- α (50 U/ml) and TNF- α (10ng/ml). Expression profile of indicated ISGs measured by qRT-PCR.

(B) dHepaRG were treated or not for 12 h with IKK2 Inhibitor (ML120B; 10 nM) and further infected with HDV and lysed 6 days later. qRT-PCR was performed with specific primers as indicated and normalized to the housekeeping gene, PRNP. **(C)**

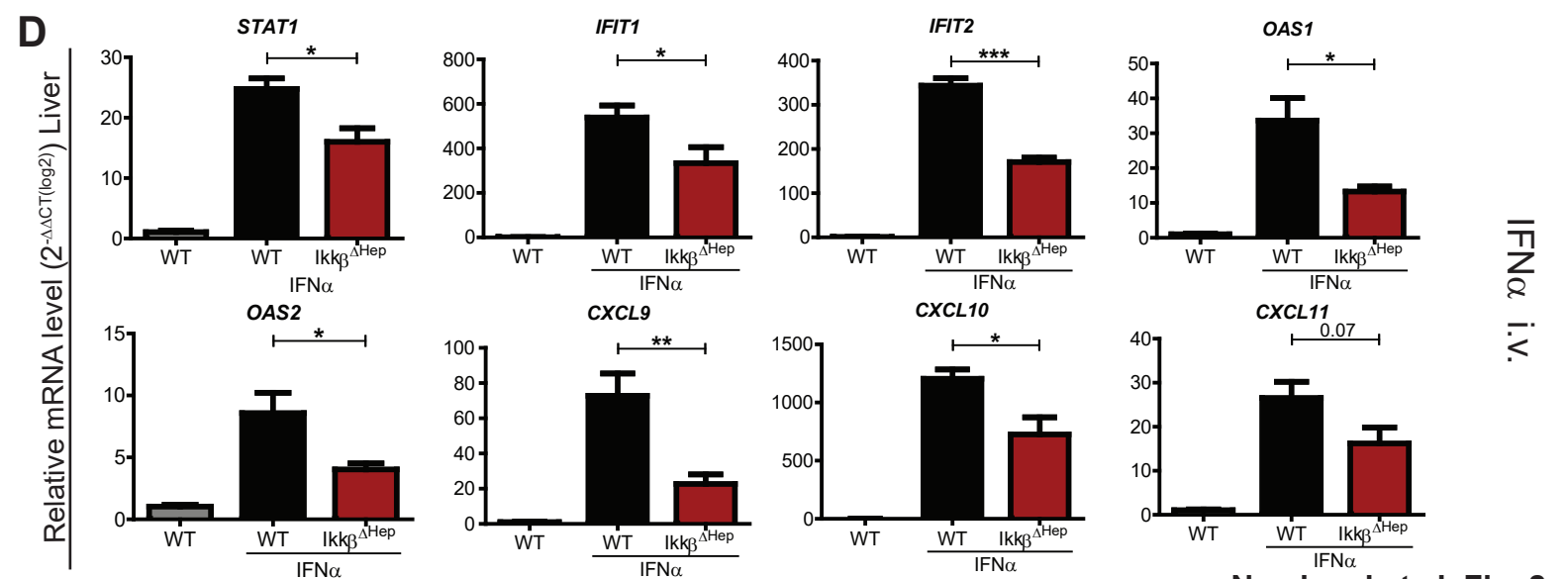
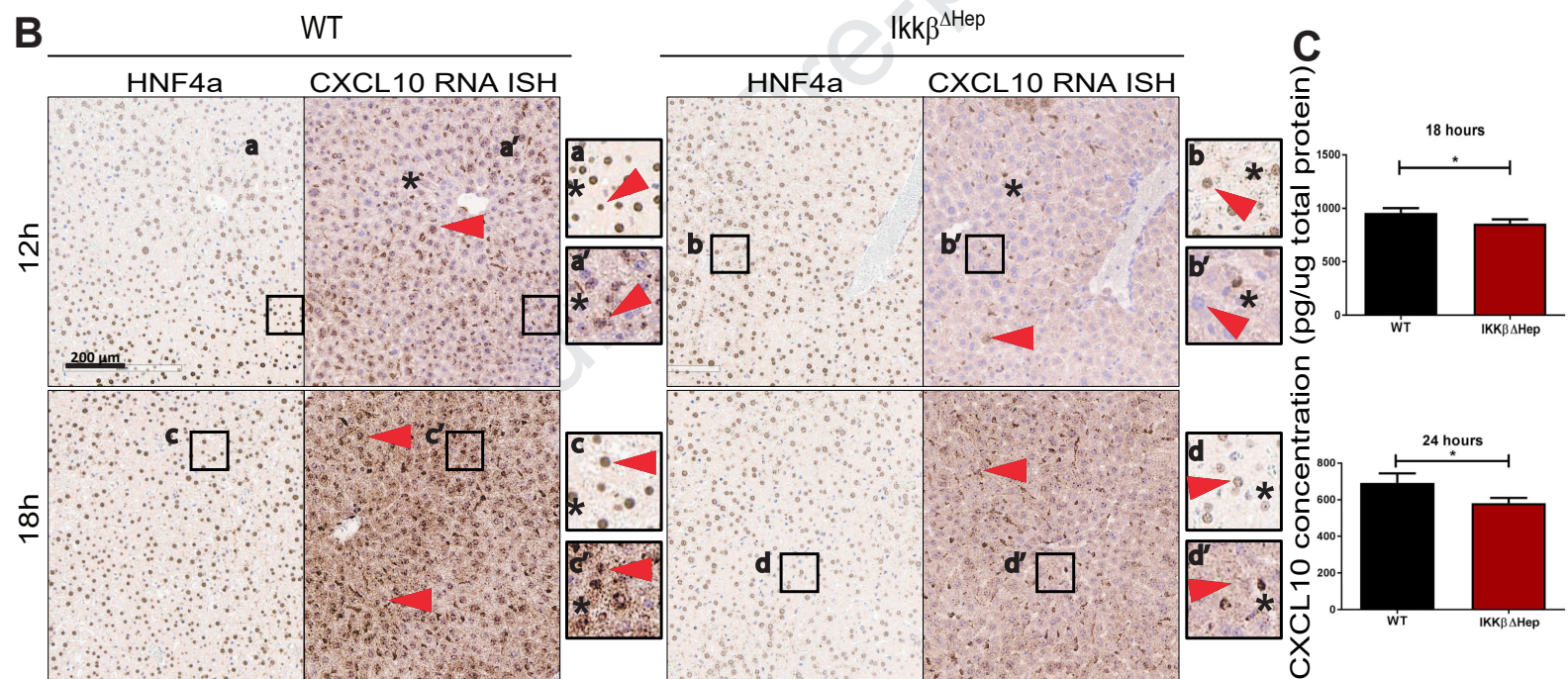
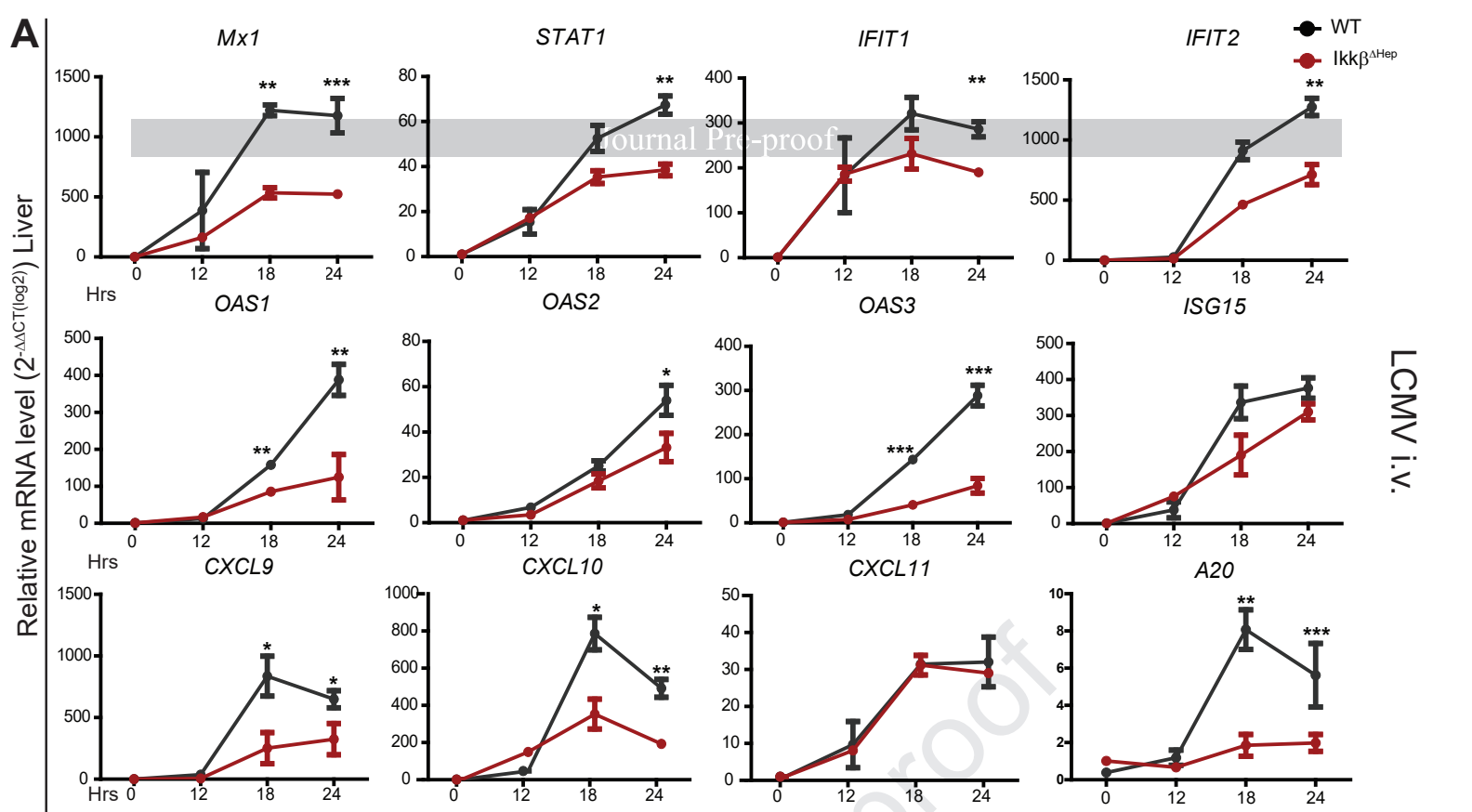
Schematic drawing of the performed experiment in **Figure D**. HepaRGs were infected with HBV. After 6 days, cells were treated with TPCA1 (10 nM). After 1 day of treatment, IFN- α (50 U/ml) was added to the medium up until day 13 p.i. **(D)** Total DNA and total RNA were extracted from dHepaRG. qRT-PCR was performed to verify the expression of ISGs. Error bars indicate mean \pm SEM, *p \leq 0.05, **p \leq 0.01, ***p \leq 0.001; unpaired Student's t-test.

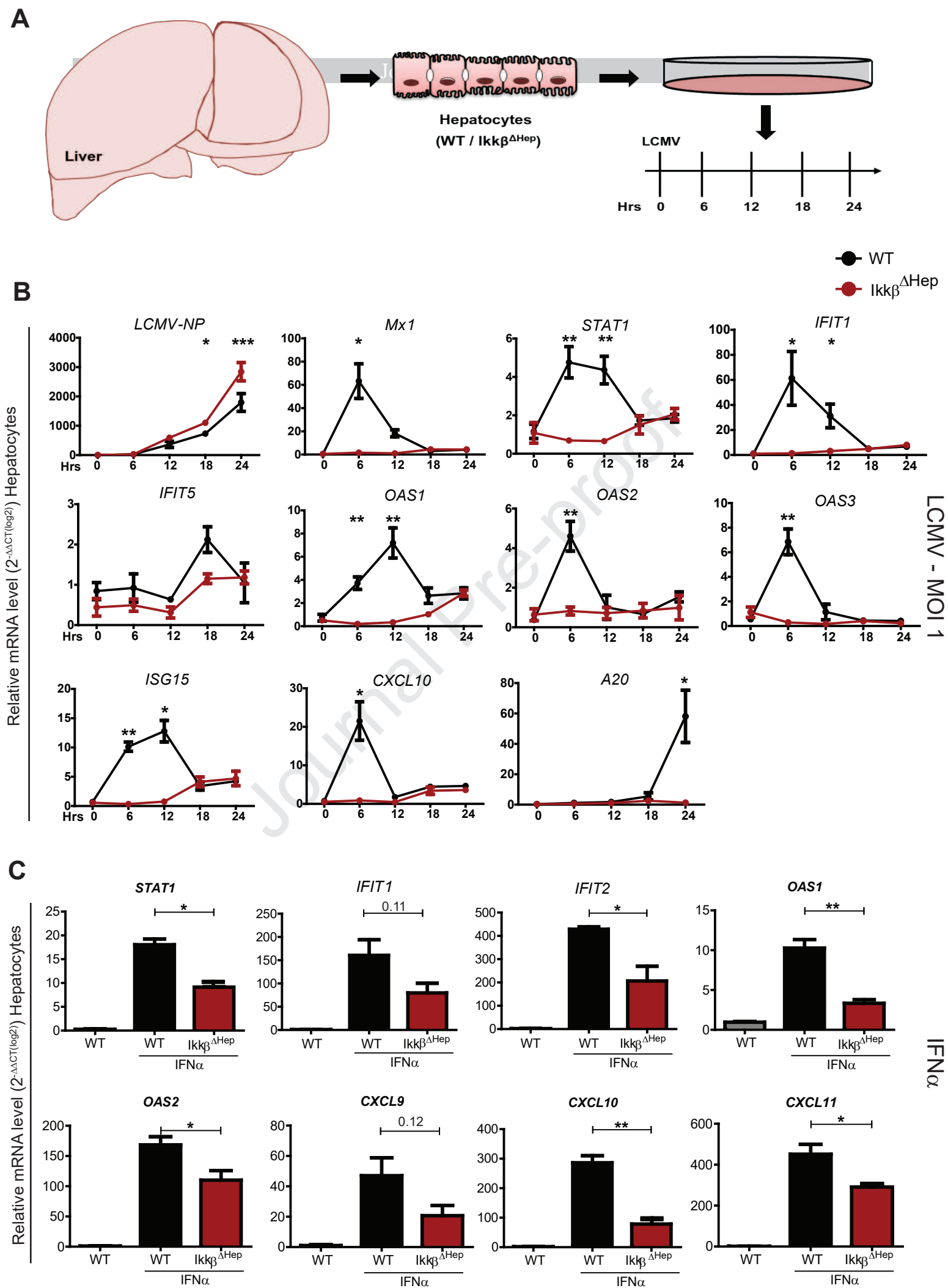
Graphical Summary – A dual role for hepatocyte intrinsic canonical NF- κ B signaling in virus control.

(Innate sensing) LCMV is sensed leading to RelA activation and nuclear translocation within hepatocytes through TLR3, TLR7, MyD88 and MAVS-dependent mechanisms and independent of TNF, TNFR1, KCs or other APCs. **(ISG expression/ innate immunity)** Lack of IKK β in hepatocytes leads to a reduced ISG response (e.g. upon LCMV infection in vitro) and a major reduction in the overall hepatic ISG production (e.g. upon LCMV infection in vivo), indicating that hepatocytes are the major producers of ISGs in the liver. In line, lack of IFNAR in hepatocytes leads to the strongest reduction of ISGs in total liver tissue upon LCMV infection. Still, Kupffer cell-derived IFNAR responses are important to support the timely and effective ISG production by hepatocytes. **(Adaptive Immunity)** During the onset of an adaptive immune response in the effector phase, IKK $\beta^{\Delta\text{Hep}}$ livers display decreased cytokine and chemokine expression as well as a decrease in the infiltration of LCMV-specific CD8⁺ T cells leading to an increased and uncontrolled virus replication in the livers. **(Virus control – effector phase)** Hepatocytes lacking IKK β and IFNAR display similar response to LCMV infection wherein virus accumulated in the hepatocytes as clusters. Hepatocytes from IFNAR $^{\Delta\text{Myel}}$ livers integrate paracrine cues from neighboring KCs and control viral replication while KCs cannot control viral replication.



Namineni et al. Fig. 1





LCMV-NP

LCMV-NP-F4/80-DAPI

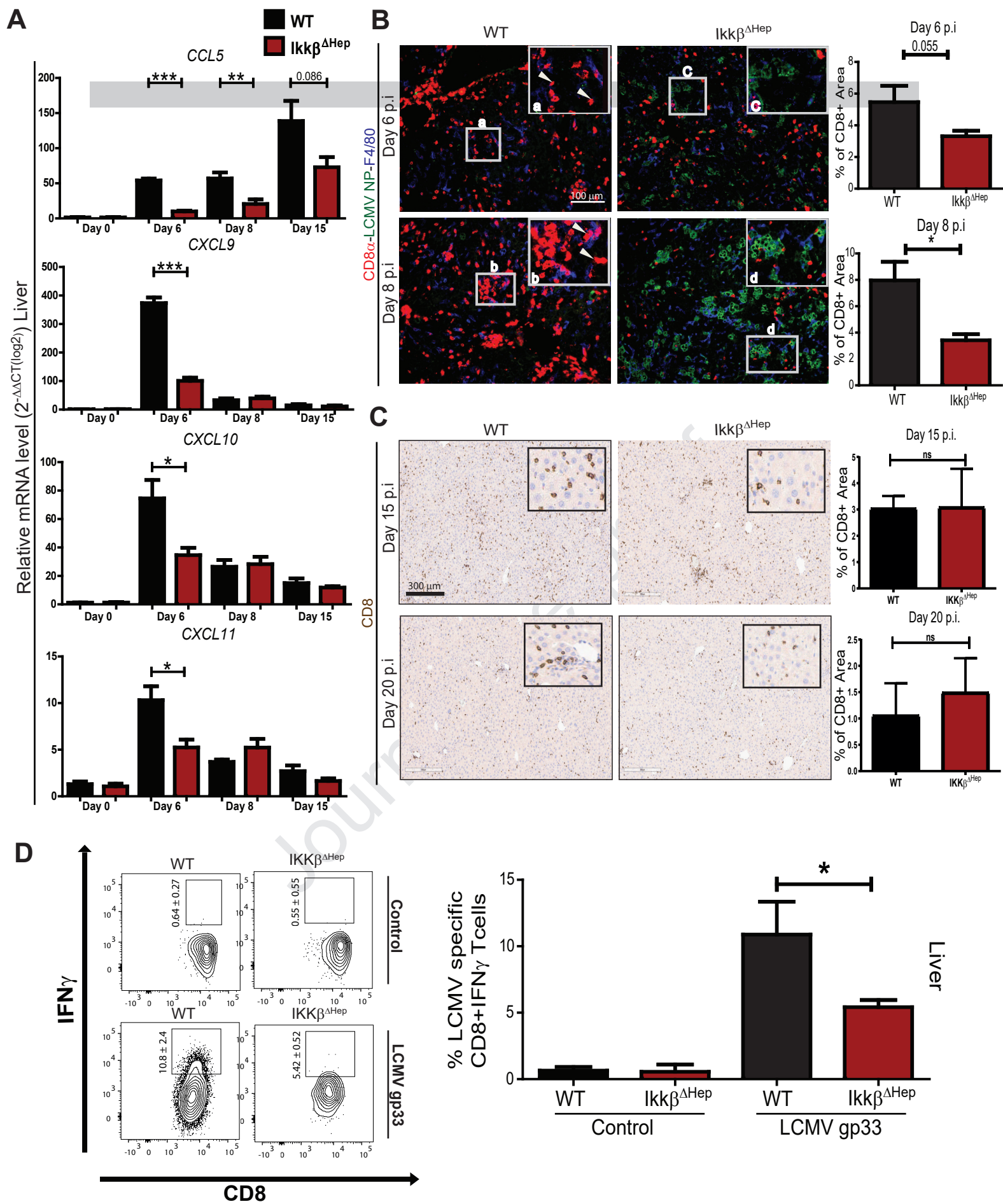
Relative mRNA level ($2^{-\Delta\Delta CT(\log 2)}$) Liver

bSTAT1

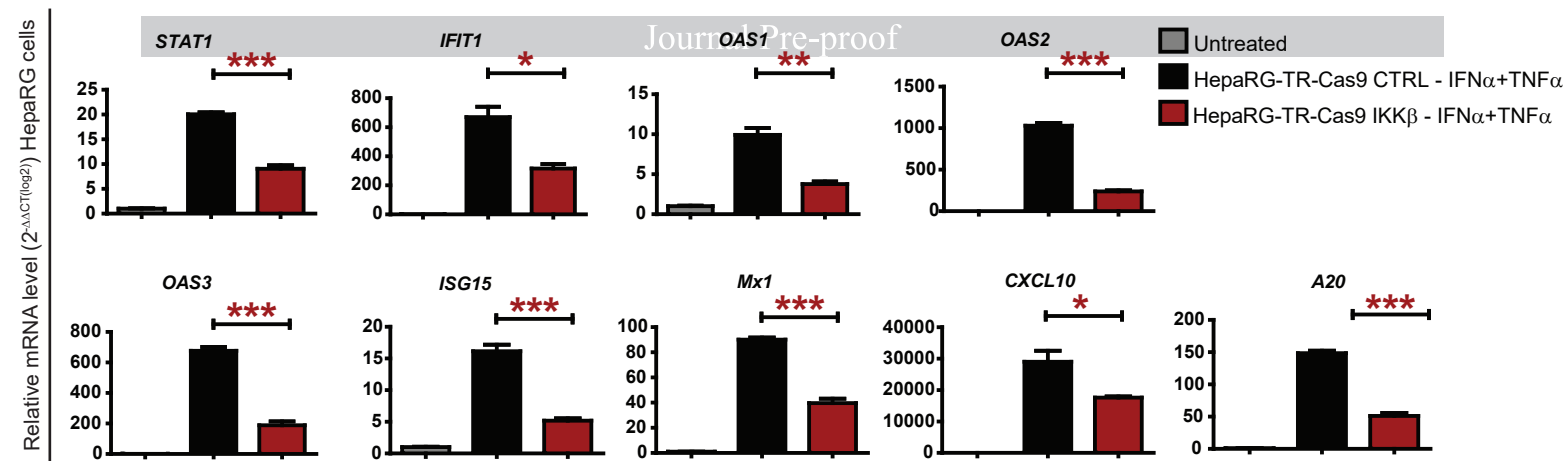
Relative mRNA level ($2^{-\Delta\Delta CT(\log 2)}$) Liver

bSTAT1

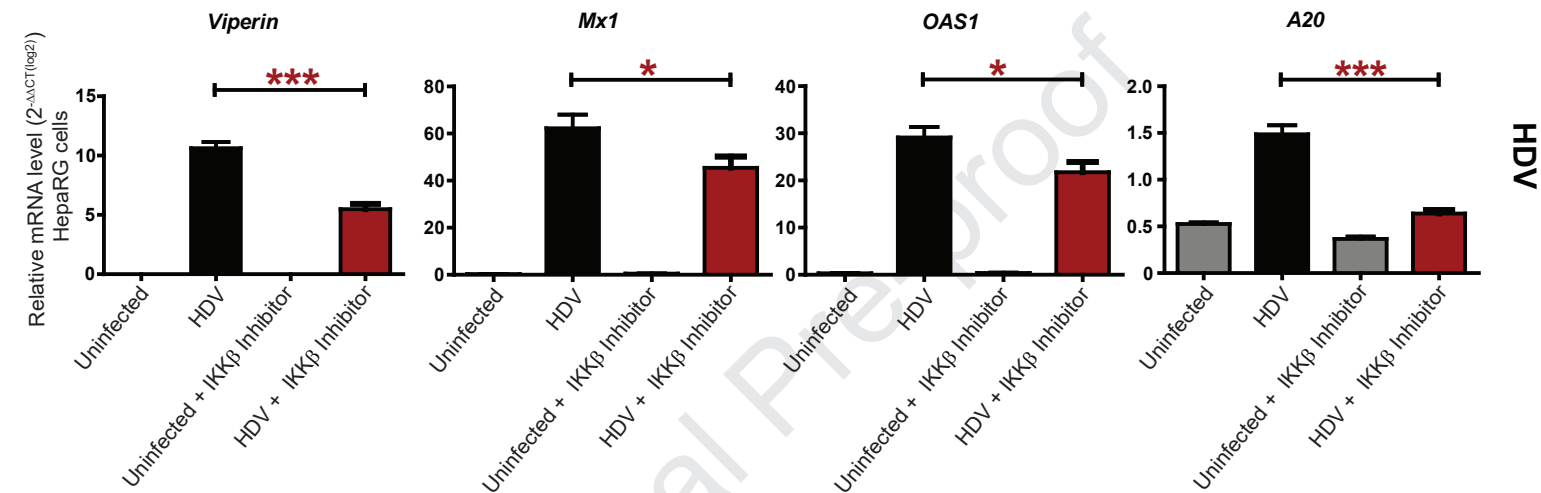




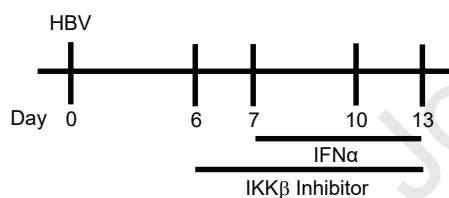
A



B



C



D

